draft, June 18, 2007

Uniformly stable numerical schemes for the Boltzmann equation preserving the compressible Navier-Stokes asymptotics

Mounir Bennoune, Mohammed Lemou, Luc Mieussens[1]

Abstract. In this paper we develop a numerical method to solve Boltzmann like equations of kinetic theory which is able to capture the compressible Navier-Stokes dynamics at small Knudsen numbers. Our approach is based on the micro/macro decomposition technique, which applies to general collision operators. This decomposition is performed in all the phase space and leads to an equivalent formulation of the Boltzmann (or BGK) equation that couples a kinetic equation with macroscopic ones. This new formulation is then discretized with a semi-implicit time scheme combined with a staggered grid space discretization. Finally, several numerical tests are presented in order to illustrate the efficiency of our approach. Incidentally, we also introduce in this paper a modification of a standard splitting method that allows to preserve the compressible Navier-Stokes asymptotics in the case of the simplified BGK model. Up to our knowledge, this property is not known for general collision operators.

Key words. Boltzmann equation, BGK equation, compressible Navier-Stokes equations, Chapman-Enskog expansion, asymptotic preserving schemes, micro-macro decomposition.

AMS subject classifications. 65M06, 35B25, 82C80, 41A60

1 Introduction

The most known kinetic model for rarefied gases is the well known Boltzmann equation (see [5] for instance). A dimensionless form of this equation is written as

$$\partial_t f + v \cdot \nabla_x f = \frac{1}{\varepsilon} Q(f, f), \quad t > 0, \quad (x, v) \in \mathbb{R}^d \times \mathbb{R}^d, \tag{1}$$

where $f(t, x, v)$ is the distribution function which depends on time $t \geq 0$, on the position of particles $x \in \mathbb{R}^d$ and on their velocity $v \in \mathbb{R}^d$. The parameter ε is the Knudsen number which measures the degree of rarefaction and is proportional to the mean free path. Finally, Q is a nonlinear collision operator describing interactions between particles. It generally acts

[1]Institut de Mathématiques de Toulouse (UMR 5219), Université Paul Sabatier, 118, Route de Narbonne, 31062 TOULOUSE cedex 9, France (bennoune@mip.ups-tlse.fr, lemou@mip.ups-tlse.fr, mieussens@mip.ups-tlse.fr).

on the velocity dependence of f only. When the number of collisions becomes very large, the mean free path (the distance travelled by a particle between two collisions) becomes small as compared to a characteristic lenght of the physical domain under consideration. In this regime a macroscopic description of the gas is more adapted. Fundamental examples are compressible Euler and compressible Navier-Stokes (CNS) equations, which describe the evolution of averaged quantities as the local density, momentum and energy of the gas. The CNS model is more accurate than the Euler equations because it gives a correction of order ε by involving terms such as viscosity and heat conductivity. However, physically, such classical fluid models could be unsufficient to correctly describe the macroscopic evolution of the gas, especially when it is far from equilibrium. Fluid models like the compressible Euler or CNS type are classically derived using the moment method in combination with perturbation methods such as Hilbert or Chapman-Enskog expansions [5], [6]. In particular, the derivation of the CNS model from Boltzmann equation in fluid regime yields an approximation of viscosity and heat fluxes in the gas up to terms of the order of ε^2.

The general context of this paper is the development of numerical schemes for solving the Boltzmann equation that are uniformly stable along the transition from kinetic regime to the fluid regime. Indeed, this property plays an important role in practical applications: plasma physics, aerospatial technology, semiconductors, neutron transport and many others. The main difficulty is due to the term $\frac{1}{\varepsilon}$ which becomes stiff when ε is close to zero (fluid regime). In this case, solving the Boltzmann equation by a standard explicit numerical scheme requires the use of a time step of the order of ε, which leads to very expensive numerical computations for small ε. To avoid this difficulty, it is necessary to use an implicit or semi-implicit time discretization for the collision part. However, due to the complicated structure of the Boltzmann collision operator, the construction of suitable implicit schemes is still a numerical challenge. In fact, such numerical schemes should also have a correct asymptotic behaviour: for small parameter ε, the schemes should degenerate into a good approximation of the fluid asymptotics (Euler or CNS equations) of the Boltzmann equation. This property is often called asymptotic preserving property.

At the level of the Euler asymptotics, many authors have proposed asymptotic preserving numerical approximations for solving the Boltzmann equation. For example, numerical schemes able to capture the correct Euler limit have been proposed in [8] in the case of the BGK equation, and then for more general kinetic equations in [16, 14, 3, 27, 28]. The case of the diffusion scaling has also been investigated in a series of works, see [18, 19, 21, 17, 15, 26]. In the same spirit, we also mention the work on the incompressible Navier-Stokes limit developped in [20].

Many numerical methods for kinetic equations are based on a splitting method which consists in solving the collision and the transport part separately. For the BGK model, it is known (see [8]) that an exact solving of the collision part allows to obtain a correct Euler limit when ε goes to zero. Here, we propose in this paper a slight modification of this method allowing to also capture the CNS asymptotics corresponding to the BGK model. In the case of the quadratic Boltzmann operator, the Euler asymptotic preserving property can be ensured using the so-called Wild sums [14, 27, 28]. However, it seems that this method

is not able to capture the CNS asymptotics for small ε. In fact, up to our knowledge there is no numerical work treating the CNS asymptotics of a kinetic model, even for simplified models like the BGK equation.

We mention that another strategy to decrease the computational cost of a kinetic simulation consists in coupling the Boltzmann equation with fluid models (Euler, Navier-Stokes, or diffusion model) (see [23, 9, 10, 11]) for example). This strategy is based on a domain decomposition aiming at solving kinetic and macroscopic equations simultaneously on different subdomains. However, the efficiency of such techniques can be improved by using asymptotic preserving schemes, in particular near the interface (see [10]).

In this paper, we present a deterministic method based on a decomposition of the Boltzmann equation into a system coupling a kinetic equation with a fluid one. The fluid part of this system degenerates, for small ε, into the CNS equations, up to $O(\varepsilon^2)$, while the kinetic part remains uniformly stable with respect to ε. We emphasize that our approach does not need any approximation and any domain decomposition method neither for space variable nor for velocity. Our strategy is as follows. We decompose the distribution function $f = f(t, x, v)$ into the sum of its Maxwellian $M(U)$ and $g = \frac{f - M(U)}{\varepsilon}$:

$$f = M(U) + \varepsilon g, \tag{2}$$

where U is the vector of the first moments of f (density, momentum and energy):

$$U = \int_{\mathbb{R}^d} \begin{pmatrix} 1 \\ v \\ \frac{1}{2}|v|^2 \end{pmatrix} f(v) dv = \begin{pmatrix} \rho \\ \rho u \\ \frac{1}{2}\rho|u|^2 + \frac{d}{2}\rho T \end{pmatrix}, \tag{3}$$

and $M(U)$ is defined as

$$M(U)(v) = \frac{\rho}{(2\pi T)^{\frac{d}{2}}} \exp\Big(- \frac{|v-u|^2}{2T} \Big). \tag{4}$$

Inserting the micro-macro decomposition (2) into equation (1), we show that g and U must satisfy a coupled system of equations which is equivalent to the original Boltzmann equation (1). This system is composed of a kinetic equation on g and a macroscopic equation on U. As we will show in this paper, using a time semi-implicit scheme on this formulation naturally leads to an asymptotic preserving scheme at the level of the CNS asymptotics. Note that a similar approach has been proposed in [13] to design fluid models with localized kinetic upscaling effects. But the construction of asymptotic preserving schemes was not studied there.

We point out that our method extends to more general collision operators of Boltzmann type and that it can be simply generalized to get asymptotic preserving schemes at higher orders in ε (Burnett like approximations). Also note that our approach also applies to diffusion limits of kinetic equations as shown in [24]. Finally, we mention that some ideas presented in this paper have already been proposed in [22] for the construction of asymptotic preserving schemes for the radiative heat transfer equation.

The outline of this paper is the following: in the next section, we present a brief review of the Boltzmann and BGK equations, and their Euler and Navier-Stokes asymptotics. In section 3, using the micro-macro decomposition, we construct the equivalent system to the Boltzmann equation and prove formally that it gives the CNS equations up to $O(\varepsilon^2)$. Section 4 is concerned with the numerical approximation of such constructed system, where the time and space discretizations are separately detailed. In section 5, we review some other standard numerical schemes used for solving the Boltzmann-BGK equation and discuss their properties regarding the CNS asymptotics. Finally, we give in section 6 several classical numerical tests in order to illustrate the efficiency of our method in a one dimensional setting.

2 The Boltzmann equation and its fluid approximations

2.1 The Boltzmann equation

We consider the usual Boltzmann equation (see [4] for details) in the dimensionless form, with an initial data

$$\partial_t f + v \cdot \nabla_x f = \frac{1}{\varepsilon} Q(f,f), \quad t > 0, (x,v) \in \mathbb{R}^d \times \mathbb{R}^d, \tag{5}$$

$$f(t=0,x,v) = f_0(x,v), \tag{6}$$

where the collision operator Q is a bilinear functional and acts only on the velocity dependance of the distribution function f. In all what follows, we use the notations

$$m(v) = (1, v, \frac{|v|^2}{2})^T, \quad \text{and} \quad \langle g \rangle = \int_{\mathbb{R}^d} g(v)\, dv \tag{7}$$

for any scalar or vector function $g = g(v)$. The Boltzmann operator $Q(f,f)$ has important physical properties as:

1. local conservation of mass, momentum and energy

$$\langle m Q(f,f) \rangle = 0, \quad \forall f \geq 0. \tag{8}$$

2. The entropy inequality

$$\langle Q(f,f) \log(f) \rangle \leq 0, \quad \forall f \geq 0.$$

3. The non-negative equilibrium functions f, i.e., such that $Q(f,f) = 0$, are the Maxwellian distributions given by

$$M(U)(v) = \frac{\rho}{(2\pi T)^{\frac{d}{2}}} \exp\Big(- \frac{|v-u|^2}{2T} \Big), \tag{9}$$

where ρ, u and T are density, mean velocity and temperature associated to U by the relation

$$\langle mM(U)\rangle = U = (\rho, \rho u, \frac{1}{2}\rho|u|^2 + \frac{d}{2}\rho T). \tag{10}$$

Usually, to avoid the complexity of the Boltzmann collision operator, the simpler BGK model is considered (see [5] for instance)

$$\partial_t f + v \cdot \nabla_x f = \frac{1}{\varepsilon\tau}(M(U) - f), \tag{11}$$

where U is the vector whose components are the first moments of f according to expression (3), and τ is a relaxation time that may depend on ρ and T. Conservation of mass, momentum and energy as well as the entropy inequality are readily satisfied by the BGK model. The Maxwellians are clearly the equilibrium functions associated to the BGK collision operator.

2.2 Conservation laws and asymptotic fluid models

The physical conservation laws of mass, momentum and energy can be expressed from (5) by using the moment method. For this, we multiply the Boltzmann equation (5) by the vector of locally conserved quantities, i.e., by $m(v)$ given by (7), and then integrate with respect to v. Using the conservation property of Q, this gives:

$$\partial_t \langle mf\rangle + \nabla_x \cdot \langle vmf\rangle = 0.$$

This is equivalent to the following non closed system of conservation laws

$$\partial_t \begin{pmatrix} \rho \\ \rho u \\ E \end{pmatrix} + \nabla_x \cdot \begin{pmatrix} \rho u \\ \rho u \otimes u + \mathbb{P} \\ Eu + \mathbb{P}u + \mathbb{Q} \end{pmatrix} = 0, \tag{12}$$

where $E = \frac{1}{2}\rho|u|^2 + \frac{d}{2}\rho T$ is the energy, $\mathbb{P} = \langle (v-u)\otimes(v-u)f\rangle$ is the pressure tensor, and $\mathbb{Q} = \frac{1}{2}\langle (v-u)|v-u|^2 f\rangle$ is the heat flux vector. When ε goes to 0 in (5), the distribution function f tends to a local Maxwellian $M(U)$. Therefore, system (12) can be approximated by a closed system on U by using expression (9). Within this approximation, the pressure tensor $\mathbb{P}$ and the heat flux vector $\mathbb{Q}$ are given by

$$\mathbb{P} = pI, \quad \mathbb{Q} = 0,$$

where $p = \rho T$ is the pressure, and I is the identity matrix. Then (12) reduces to the usual compressible Euler equations

$$\partial_t \begin{pmatrix} \rho \\ \rho u \\ E \end{pmatrix} + \nabla_x \cdot \begin{pmatrix} \rho u \\ \rho u \otimes u + pI \\ (E+p)u \end{pmatrix} = 0. \tag{13}$$

It is well known that a first order correction (in ε) to the Euler equations can be derived by using the classical Chapman-Enskog expansion. This correction is nothing but the CNS system

$$\partial_t \begin{pmatrix} \rho \\ \rho u \\ E \end{pmatrix} + \nabla_x \cdot \begin{pmatrix} \rho u \\ \rho u \otimes u + pI \\ (E+p)u \end{pmatrix} = -\varepsilon \begin{pmatrix} 0 \\ \nabla_x \cdot \sigma \\ \nabla_x \cdot (\sigma u + q) \end{pmatrix}. \tag{14}$$

In these equations, the pressure tensor is $\mathbb{P} = pI + \sigma$ where $\sigma = -\mu\Big(\nabla_x u + (\nabla_x u)^T - \frac{2}{d}\nabla_x \cdot uI\Big)$ is the stress tensor, while the heat flux is $\mathbb{Q} = \varepsilon q = -\varepsilon\kappa\nabla_x T$. In these relations, μ and κ are functions of U and are the so-called viscosity and heat conductivity coefficients, see [1] and the references therein for details. In the following section, we perform the Chapman-Enskog procedure in the context of our micro-macro decomposition.

3 A kinetic/fluid formulation of the Boltzmann equation

In this section we show that the Boltzmann equation can be equivalently written as a system coupling a hydrodynamic part with a kinetic part of the distribution function. This formulation is the basis of our numerical method (see section 4).

3.1 Micro-Macro decomposition

Assume that f satisfies the Boltzmann equation (5). We decompose f as follows

$$f = M(U) + \varepsilon g, \tag{15}$$

where U is linked to f by (3) and $M(U)$ is the associated Maxwellian according to (4). When no confusion is possible, we set $M(U) = M$. Inserting decomposition (15) into (5), we obtain

$$\partial_t M + v \cdot \nabla_x M + \varepsilon(\partial_t g + v \cdot \nabla_x g) = \frac{1}{\varepsilon} Q(M + \varepsilon g, M + \varepsilon g).$$

Since Q is a bilinear and $Q(M, M) = 0$, we have

$$Q(M + \varepsilon g, M + \varepsilon g) = Q(M, M) + 2\varepsilon Q(M, g) + \varepsilon^2 Q(g, g) = \varepsilon \mathcal{L}_M g + \varepsilon^2 Q(g, g),$$

where $\mathcal{L}_M$ is the linearized collision operator given by

$$\mathcal{L}_M g = 2Q(M, g).$$

Thus, we get

$$\partial_t M + v \cdot \nabla_x M + \varepsilon(\partial_t g + v \cdot \nabla_x g) = \mathcal{L}_M g + \varepsilon Q(g, g). \tag{16}$$

Now, we use a projection technique to separate the macroscopic and microscopic quantities M and g. Consider the Hilbert space $L^2_M = \{\varphi \text{ such that } \varphi M^{-\frac{1}{2}} \in L^2(\mathbb{R}^d)\}$ endowed with the weighted scalar product

$$(\varphi, \psi)_M = \left\langle \varphi \psi M^{-1} \right\rangle .$$

It is well known that $\mathcal{L}_M$ is a non-positive self-adjoint operator on L^2_M and that its null space is $\mathcal{N}(\mathcal{L}_M) = \text{Span}\{M, vM, |v|^2 M\}$. Let Π_M be the orthogonal projection in L^2_M onto $\mathcal{N}(\mathcal{L}_M)$. After easy computations in the orthogonal basis

$$\mathcal{B} = \left\{ \frac{1}{\rho} M, \frac{(v-u)}{\sqrt{T}} \frac{1}{\rho} M, \left(\frac{|v-u|^2}{2T} - \frac{d}{2} \right) \frac{1}{\rho} M \right\} \tag{17}$$

of the space $\mathcal{N}(\mathcal{L}_M)$, one finds for any function $\varphi \in L^2_M$ the following expression of $\Pi_M(\varphi)$:

$$\Pi_M(\varphi) = \frac{1}{\rho} \left[\langle \varphi \rangle + \frac{(v-u) \cdot \langle (v-u)\varphi \rangle}{T} + \left(\frac{|v-u|^2}{2T} - \frac{d}{2} \right) \frac{2}{d} \left\langle \left(\frac{|v-u|^2}{2T} - \frac{d}{2} \right) \varphi \right\rangle \right] M.$$

Now, we prove the following elementary properties of Π_M:

Lemma 3.1. *If M and g are defined as in (15) then we have*

$$(I - \Pi_M)(\partial_t M) = \Pi_M(g) = \Pi_M(\partial_t g) = \Pi_M(Q(g,g)) = \Pi_M(\mathcal{L}_M g) = 0.$$

Proof. Since

$$\partial_t M = \left[\frac{\partial_t \rho}{\rho} + \frac{v-u}{T} \cdot \partial_t u + \left(\frac{|v-u|^2}{2T^2} - \frac{d}{2T} \right) \partial_t T \right] M$$

clearly belongs to $\mathcal{N}(\mathcal{L}_M)$ (see (17)), then $\Pi_M(\partial_t M) = \partial_t M$.

Moreover, thanks to (15) we have $\langle mg \rangle = \frac{1}{\varepsilon} \langle m(f - M) \rangle = 0$ and hence $\langle m(\partial_t g) \rangle = \partial_t \langle mg \rangle = 0$. This implies $\Pi_M(g) = 0$ and $\Pi_M(\partial_t g) = 0$. Finally, the conservation properties (8) of Q imply that $\Pi_M(Q(g,g)) = 0$. It is classical to deduce that $\mathcal{L}_M$ satisfies the same properties $\langle m \mathcal{L}_M g \rangle = 0$ and hence $\Pi_M(\mathcal{L}_M g) = 0$. □

We now apply the orthogonal projection $I - \Pi_M$ to (16) to obtain

$$(I - \Pi_M)(\partial_t M + v \cdot \nabla_x M) + \varepsilon (I - \Pi_M)(\partial_t g + v \cdot \nabla_x g) = (I - \Pi_M)\mathcal{L}_M g + \varepsilon (I - \Pi_M) Q(g,g).$$

Then using lemma 3.1, we get the following equation on g

$$\partial_t g + (I - \Pi_M)(v \cdot \nabla_x g) - Q(g,g) = \frac{1}{\varepsilon} \big[\mathcal{L}_M g - (I - \Pi_M)(v \cdot \nabla_x M) \big]. \tag{18}$$

Now, taking the moments of equation (16) and using again lemma 3.1, we get

$$\partial_t \langle mM \rangle + \nabla_x \cdot \langle vmM \rangle + \varepsilon \nabla_x \cdot \langle vmg \rangle = 0.$$

Let $F(U) = \langle vmM \rangle$ be the flux vector of $U = \langle mM \rangle$, then the previous equation reads

$$\partial_t U + \nabla_x \cdot F(U) + \varepsilon \nabla_x \cdot \langle vmg \rangle = 0. \tag{19}$$

Therefore, the coupled system (18)-(19) provides a kinetic/fluid formulation of the Boltzmann equation. This last formulation is in fact equivalent to the Boltzmann equation (5) as stated in the following proposition.

Proposition 3.1. *(i) Let f be a solution of the Boltzmann equation (5) with initial data (6), and $M = M(U)$ its associated Maxwellian according to (3)–(4). Then the pair (U, g), where $U = \langle mf \rangle$ and $g = \frac{1}{\varepsilon}(f - M)$, is a solution to the coupled system (18)-(19) with the associated initial data*

$$U(t = 0) = U_0 = \langle mf_0 \rangle \qquad \text{and} \qquad g(t = 0) = \frac{1}{\varepsilon}(f_0 - M(U_0)). \tag{20}$$

(ii) Conversely, if (U, g) satisfies system (18)-(19) with initial data (U_0, g_0) such that $\langle mg_0 \rangle = 0$, then $f = M(U) + \varepsilon g$ is a solution to the Boltzmann equation (5) with initial data $f_0 = M(U_0) + \varepsilon g_0$ and we have $U = \langle mf \rangle$ and $\langle mg \rangle = 0$.

Proof. The proof of (i) is nothing but the construction of the coupled system (18)-(19) detailed above. For (ii), consider (U, g) a solution of (18)-(19). We set $f = M + \varepsilon g$, where M is the Maxwellian asociated to U, and show that f satisfies the Boltzmann equation. From (18), we have

$$\varepsilon \partial_t g + v \cdot \nabla_x f = \mathcal{L}_M g + \varepsilon Q(g, g) + \Pi_M (v \cdot \nabla_x f),$$

and consequently

$$\partial_t f + v \cdot \nabla_x f = \frac{1}{\varepsilon} Q(f, f) + \Pi_M (v \cdot \nabla_x f) + \partial_t M. \tag{21}$$

The term $\Pi_M(v \cdot \nabla_x f) + \partial_t M$ belongs to $\mathcal{N}(\mathcal{L}_M)$ as a sum of two elements of $\mathcal{N}(\mathcal{L}_M)$. On the other hand, since equation (19) is equivalent to $\langle m(\Pi_M(v \cdot \nabla_x f) + \partial_t M) \rangle = 0$, this implies that $\Pi_M(v \cdot \nabla_x f) + \partial_t M$ is orthogonal to $\mathcal{N}(\mathcal{L}_M)$. Consequently, $\Pi_M(v \cdot \nabla_x f) + \partial_t M = 0$, and f satisfies the Boltzmann equation from (21). The property $\langle mg \rangle = 0$ is simply obtained by applying Π_M to (18) and then by using the property of the initial data. □

The following proposition gives a similar result in the case of the one-dimensional ($d = 1$) BGK model.

Proposition 3.2. *With the previous notations, $f = M(U) + \varepsilon g$ is a solution of the BGK equation (11) with initial data (6) if and only if (U, g) satisfies the system*

$$\partial_t g + (I - \Pi_M)(v \partial_x g) = -\frac{1}{\varepsilon} \Big[\frac{1}{\tau} g + (I - \Pi_M)(v \partial_x M) \Big], \tag{22}$$

$$\partial_t U + \partial_x F(U) + \varepsilon \partial_x \langle vmg \rangle = 0. \tag{23}$$

with initial data (20).

Note that in case of a boundary value problem, using the micro-macro decomposition (15) may induce some difficulties. In particular, at boundary points, f is generally known only for incoming velocities, and hence it may be difficult to define the macroscopic moments U in (15). In this article, we do not consider this problem and defer the treatment of boundary conditions to a future work. We refer to [24] for such a study in the case of the linear transport model.

3.2 Chapman-Enskog expansion and compressible Navier-Stokes equations

For a sake of clarity, we just show in this section how the classical Chapman-Enskog procedure applies to system (18)-(19). More precisely, we simply give the results of standard calculations as in [1], adpated to the context of our coupled kinetic/fluid formulation (18)-(19), and derive the corresponding CNS equations. This derivation is similar to the projection method used in [12].

With the previous notations and from the kinetic equation of our coupled system (18), we can write

$$\mathcal{L}_M g = (I - \Pi_M)(v \cdot \nabla_x M) + O(\varepsilon).$$

Now, after calculations, we obtain

$$(I - \Pi_M)(v \cdot \nabla_x M) = \Big(B : (\nabla_x u + (\nabla_x u)^T - \frac{2}{d}(\nabla_x \cdot u) I) + A \cdot \frac{\nabla_x T}{\sqrt{T}} \Big) M + O(\varepsilon),$$

where

$$A = \left(\frac{|v-u|^2}{2T} - \frac{d+2}{2} \right) \frac{v-u}{\sqrt{T}} \quad \text{and} \quad B = \frac{1}{2} \left(\frac{(v-u) \otimes (v-u)}{2T} - \frac{|v-u|^2}{dT} I \right).$$

It is known that $\mathcal{L}_M$ is invertible on the orthogonal of its null-space. Then, we have

$$g = \mathcal{L}_M^{-1}(BM) : (\nabla_x u + (\nabla_x u)^T - \frac{2}{d}(\nabla_x \cdot u) I) + \mathcal{L}_M^{-1}(AM) \cdot \frac{\nabla_x T}{\sqrt{T}} + O(\varepsilon).$$

Inserting this expression into the macroscopic equation (19) and using classical symmetry properties of $\mathcal{L}_M$, we get

$$\partial_t U + \nabla_x \cdot F(U) = -\varepsilon \begin{pmatrix} 0 \\ \nabla_x \cdot \sigma \\ \nabla_x \cdot (\sigma u + q) \end{pmatrix} + O(\varepsilon^2), \tag{24}$$

which is nothing but the CNS system of equations (14), up to $O(\varepsilon^2)$. The rescaled viscosity tensor and heat flux are given by

$$\sigma = -\mu \Big(\nabla_x u + (\nabla_x u)^T - \frac{2}{d} \nabla_x \cdot u I \Big), \tag{25}$$

$$q = -\kappa \nabla_x T. \tag{26}$$

The coefficients μ and κ are the viscosity and heat conductivity coefficients that only depend on the temperature, and whose general expressions can be found in [1].

In the case of the BGK model (11) for one dimensional space and velocity variables ($d = 1$), the computations are much simpler, and we obtain the corresponding CNS equations

$$\partial_t \begin{pmatrix} \rho \\ \rho u \\ E \end{pmatrix} + \partial_x \begin{pmatrix} \rho u \\ \rho u^2 + \rho T \\ Eu + \rho T u \end{pmatrix} = \varepsilon \partial_x \begin{pmatrix} 0 \\ 0 \\ \kappa \partial_x T \end{pmatrix}, \tag{27}$$

where the heat conductivity coefficient is

$$\kappa = \tau \frac{3}{2} \rho T.$$

Note that in this case, there is no diffusion term in the momentum equation.

4 Numerical approximation

Starting from the approach presented above, we are going in this section to construct a numerical approximation of system (18)-(19) for the Boltzmann equation, as well as of sytem (22)-(23) in the case of the BGK model. Our goal is to provide numerical approximations to these systems that give, for fixed time and space grid steps and up to $O(\varepsilon^2)$, a numerical scheme for the corresponding CNS equations. In that sense, the so obtained numerical schemes for Boltzmann or BGK equations are "Asymptotic Preserving" for the CNS asymptotics.

4.1 Implicit time discretization

In this first step, we present a time discretization of our coupled system (18)-(19). Space and velocity discretizations are studied in the next section. To that purpose, we denote by Δt a fixed time step, and by t_n a discrete time such that $t_n = n\Delta t,\ n \in \mathbb{N}$. We first develop the strategy in the case of the Boltzmann equation (5). Let $(U^n)_n$ and $(g^n)_n$ be two sequences that approximate U and g respectively, that is: $U^n(x) \approx U(t_n, x), \quad g^n(x, v) \approx g(t_n, x, v)$. The idea of our time discretization is the following. In equation (18), the only term which presents a stiffness in the collision part, for small ε, is $\varepsilon^{-1}\mathcal{L}_M g$. Hence, we take an implicit discretization for this term, while the term $(I - \Pi_M)(v \cdot \nabla_x M)$ is still explicit. Thus, we obtain the following discretization:

$$\frac{g^{n+1} - g^n}{\Delta t} + (I - \Pi_{M^n})(v \cdot \nabla_x g^n) - Q(g^n, g^n) = \frac{1}{\varepsilon}\Big[\mathcal{L}_{M^n} g^{n+1} - (I - \Pi_{M^n})(v \cdot \nabla_x M^n)\Big], \tag{28}$$

where $M^n = M(U^n)$ is the Maxwellian associated with the vector moment U^n according to (9)-(10). Note that g^{n+1} is uniquely determined from (28) since the operator $(I - (\Delta t/\varepsilon)\mathcal{L}_{M^n})$ is clearly invertible (see the properties of $\mathcal{L}_M$ mentioned in section 3.1). In the case of the

Boltzmann equation, the calculation of this inverse will be treated in a future work. In the present paper, all the numerical tests are done with the BGK model for which $\mathcal{L}_M$ is diagonal and hence easily invertible.

Now, we look for the time approximation of the fluid part (19) in our system. The flux $F(U)$ at time t_n is naturally approximated by $F(U^n) = \langle vmM^n \rangle$. On the other hand, in order to have diffusive terms that are evaluated at time t_n, the term $\nabla_x \cdot \langle vmg \rangle$ is discretized by $\nabla_x \cdot \langle vmg^{n+1} \rangle$. Then we have

$$\frac{U^{n+1} - U^n}{\Delta t} + \nabla_x \cdot F(U^n) + \varepsilon \nabla_x \cdot \left\langle vmg^{n+1} \right\rangle = 0. \tag{29}$$

Proposition 4.1. *(i) The time discretization (28)-(29) of the Boltzmann equation (5) gives at the limit $\varepsilon \to 0$ a scheme which is consistent with the Euler equations (13).*

(ii) Moreover, for small ε, scheme (28)-(29) is asymptotically equivalent, up to $O(\varepsilon^2)$, to an explicit time discretization of the CNS equations (14).

Proof. The asymptotic behavior of scheme (28)-(29) is obtained similary as in subsection 3.2. Indeed, from (29), we see that when $\varepsilon \to 0$, we obtain

$$\frac{U^{n+1} - U^n}{\Delta t} + \nabla_x \cdot F(U^n) = 0,$$

which is a time explicit discretization of the Euler system (13). Now, we note that from the properties of $\mathcal{L}_M$ mentionned above, the operator $(I - (\Delta t/\varepsilon)\mathcal{L}_M)$ is also invertible for all $\varepsilon \geq 0$ and $\Delta t \geq 0$. Hence, (28) yields

$$g^{n+1} = \left(I - \frac{\Delta t}{\varepsilon}\mathcal{L}_{M^n}\right)^{-1} \left[g^n - \frac{\Delta t}{\varepsilon}(I - \Pi_{M^n})(v \cdot \nabla_x M^n) - \Delta t (I - \Pi_{M^n})(v \cdot \nabla_x g^n) + \Delta t\, Q(g^n, g^n) \right].$$

Observing that $\left(I - \frac{\Delta t}{\varepsilon}\mathcal{L}_{M^n}\right)^{-1} = -\frac{\varepsilon}{\Delta t}\mathcal{L}_{M^n}^{-1} + O(\varepsilon^2)$, we get

$$g^{n+1} = \mathcal{L}_{M^n}^{-1}\left[(I - \Pi_{M^n})(v \cdot \nabla_x M^n)\right] + O(\varepsilon).$$

It follows that (29) can be written as

$$\frac{U^{n+1} - U^n}{\Delta t} + \nabla_x \cdot F(U^n) + \varepsilon \nabla_x \cdot \left\langle vm\mathcal{L}_{M^n}^{-1}\left[(I - \Pi_{M^n})(v \cdot \nabla_x M^n)\right] \right\rangle = O(\varepsilon^2). \tag{30}$$

If we neglect the $O(\varepsilon^2)$ terms, then the same computations as in section 3.2 show that (30) is indeed a time-explicit discretization of the CNS equations (14). Indeed, the $O(\varepsilon)$ term is

$$\nabla_x \cdot \left\langle vm\mathcal{L}_{M^n}^{-1}\left[(I - \Pi_{M^n})(v \cdot \nabla_x M^n)\right] \right\rangle = \Delta t \begin{pmatrix} 0 \\ \nabla_x \cdot \sigma^n \\ \nabla_x \cdot (\sigma^n u^n + q^n) \end{pmatrix},$$

where σ^n and q^n are related to U^n according to (25)-(26). □

Now, applying the same time discretization to the one dimensional ($d = 1$) BGK model, we obtain a similar result:

Proposition 4.2. *The following time discretization of the BGK equation (11)*

$$\frac{g^{n+1} - g^n}{\Delta t} + (I - \Pi_{M^n})(v \cdot \partial_x g^n) = -\frac{1}{\varepsilon}\Big[\frac{1}{\tau^n} g^{n+1} + (I - \Pi_{M^n})(v \cdot \partial_x M^n)\Big], \tag{31}$$

$$\frac{U^{n+1} - U^n}{\Delta t} + \partial_x \cdot F(U^n) + \varepsilon \partial_x \cdot \big\langle v m g^{n+1} \big\rangle = 0, \tag{32}$$

gives at the limit $\varepsilon \to 0$ a scheme which is consistent with Euler equations (13). Moreover, it also gives up to $O(\varepsilon^2)$ a scheme which is consistent with the CNS equations (27).

In all the following, we restrict ourselves to the space discretization of (31)-(32).

4.2 Space discretization

In this section, we construct a suitable space discretization of system (31)-(32) which is asymptotically equivalent to an approximation of the one dimensional CNS equations (27) up to $O(\varepsilon^2)$. There are two main difficulties. The first one is related to the discretization of the transport term in the left-hand side of (31) in the kinetic regime ($\varepsilon \approx 1$). Indeed, to guarantee the stability of the scheme in this regime, one has to use an upwind discretization for this term. The second one is the accuracy of the approximation of the diffusion terms obtained in the asymptotic regime ($\varepsilon \ll 1$). Observing that such diffusive terms are due to $\varepsilon \langle v m g^{n+1} \rangle$ via (32), and $(I - \Pi_{M^n})(v \partial_x M^n)$ via (31), we propose to discretize these terms by using central differences defined on two staggered grids. In the following, we develop this strategy in more details.

We consider spatial grid points $x_{i+\frac{1}{2}}$, denote by x_i the center of the cell $[x_{i-\frac{1}{2}}, x_{i+\frac{1}{2}}]$, and consider a uniform space step $\Delta x = x_{i+\frac{1}{2}} - x_{i-\frac{1}{2}} = x_i - x_{i-1}$. Let U_i^n and $g_{i+\frac{1}{2}}^n$ be approximations of $U(t_n, x_i)$ and $g(t_n, x_{i+\frac{1}{2}})$, respectively. Equation (31) is approximated at grid point $x_{i+\frac{1}{2}}$: to avoid the oscillations for transport dominated flows, the transport term $(I - \Pi_{M^n})(v \partial_x g^n)$ is approximated by a first order upwind scheme

$$(I - \Pi_{M^n})(v \partial_x g^n)_{|_{x_{i+\frac{1}{2}}}} \approx (I - \Pi^n_{i+\frac{1}{2}})\Big[\frac{\Phi_{i+\frac{1}{2}}(g^n) - \Phi_{i-\frac{1}{2}}(g^n)}{\Delta x}\Big],$$

where

$$\Phi_{i+\frac{1}{2}}(g) = v^+ g_{i+\frac{1}{2}} + v^- g_{i+\frac{3}{2}}. \tag{33}$$

However, the transport term $(I - \Pi_{M^n})(v \partial_x M^n)$ is considered as a source term and approximated by central differences

$$(I - \Pi_{M^n})(v \partial_x M^n)_{|_{x_{i+\frac{1}{2}}}} \approx (I - \Pi^n_{i+\frac{1}{2}})\Big(v \frac{M^n_{i+1} - M^n_i}{\Delta x}\Big),$$

where $M_i^n = M(U_i^n)$ and $\Pi^n_{i+\frac{1}{2}}$ is an approximation of $\Pi_{M(U(t_n,x_{i+\frac{1}{2}}))}$ that will be given below. This leads to the following approximation of (31)

$$\begin{aligned}&\frac{g^{n+1}_{i+\frac{1}{2}} - g^n_{i+\frac{1}{2}}}{\Delta t} + (I - \Pi^n_{i+\frac{1}{2}})\Big[v^+\frac{g^n_{i+\frac{1}{2}} - g^n_{i-\frac{1}{2}}}{\Delta x} + v^-\frac{g^n_{i+\frac{3}{2}} - g^n_{i+\frac{1}{2}}}{\Delta x}\Big]\\ &\quad = -\frac{1}{\varepsilon}\big[g^{n+1}_{i+\frac{1}{2}} + (I - \Pi^n_{i+\frac{1}{2}})(v\frac{M^n_{i+1} - M^n_i}{\Delta x})\big]. \qquad (34)\end{aligned}$$

Now, the fluid equation (32) is approximated at points x_i. First, the discretization of the flux $\partial_x F(U^n)$ can be done by any classical scheme:

$$\partial_x F(U^n)_{|_{x_i}} \approx \frac{F_{i+\frac{1}{2}}(U^n) - F_{i-\frac{1}{2}}(U^n)}{\Delta x}.$$

For instance, in the kinetic context, a natural scheme could be the first order kinetic flux vector splitting of Deshpande-Pullin [25]:

$$F_{i+\frac{1}{2}}(U^n) = \left\langle m(v^+ M^n_i + v^- M^n_{i+1})\right\rangle. \qquad (35)$$

The non-equilibrium flux $\partial_x \langle vmg^{n+1}\rangle$ is approximated by central differences as

$$\partial_x \left\langle vmg^{n+1}\right\rangle \approx \frac{1}{\Delta x}\left\langle vm\Big(g^{n+1}_{i+\frac{1}{2}} - g^{n+1}_{i-\frac{1}{2}}\Big)\right\rangle.$$

Thus, we obtain the following approximation of (32):

$$\frac{U^{n+1}_i - U^n_i}{\Delta t} + \frac{F_{i+\frac{1}{2}}(U^n) - F_{i-\frac{1}{2}}(U^n)}{\Delta x} = -\varepsilon\left\langle vm\frac{g^{n+1}_{i+\frac{1}{2}} - g^{n+1}_{i-\frac{1}{2}}}{\Delta x}\right\rangle. \qquad (36)$$

Now, we investigate the formal asymptotics of the numerical scheme given by (34) and (36) when $\varepsilon \to 0$. First, from (34) we have

$$g^{n+1}_{i+\frac{1}{2}} = -(I - \Pi^n_{i+\frac{1}{2}})(v\ \frac{M^n_{i+1} - M^n_i}{\Delta x}) + O(\varepsilon),$$

and then from (36)

$$\begin{aligned}&\frac{U^{n+1}_i - U^n_i}{\Delta t} + \frac{F_{i+\frac{1}{2}}(U^n) - F_{i-\frac{1}{2}}(U^n)}{\Delta x}\\ &\quad = \frac{\varepsilon}{\Delta x}\left\langle vm\Big[(I - \Pi^n_{i+\frac{1}{2}})(v\ \frac{M^n_{i+1} - M^n_i}{\Delta x}) - (I - \Pi^n_{i-\frac{1}{2}})(v\ \frac{M^n_i - M^n_{i-1}}{\Delta x})\Big]\right\rangle + O(\varepsilon^2). \qquad (37)\end{aligned}$$

In order to get from (37) a scheme which is consistent with the CNS equations up to $O(\varepsilon^2)$, a simple calculation shows that suitable choices of $\Pi^n_{i+\frac{1}{2}}$ are

$$\Pi_{i+\frac{1}{2}} = \frac{\Pi_i + \Pi_{i+1}}{2} = \frac{\Pi(U_i) + \Pi(U_{i+1})}{2}, \quad \text{or} \quad \Pi_{i+\frac{1}{2}} = \Pi(\frac{U_i + U_{i+1}}{2}).$$

We summarize the above result in the following proposition.

Proposition 4.3. *Consider the following time and space approximation of the BGK equation (11)*

$$\frac{g^{n+1}_{i+\frac12}-g^n_{i+\frac12}}{\Delta t}+(I-\Pi^n_{i+\frac12})\Big[v^+\frac{g^n_{i+\frac12}-g^n_{i-\frac12}}{\Delta x}+v^-\frac{g^n_{i+\frac32}-g^n_{i+\frac12}}{\Delta x}\Big]$$
$$=-\frac{1}{\varepsilon}\big[g^{n+1}_{i+\frac12}+(I-\Pi^n_{i+\frac12})(v\frac{M^n_{i+1}-M^n_i}{\Delta x})\big], \tag{38}$$
$$\frac{U^{n+1}_i-U^n_i}{\Delta t}+\frac{F_{i+\frac12}(U^n)-F_{i-\frac12}(U^n)}{\Delta x}+\varepsilon\left\langle vm\frac{g^{n+1}_{i+\frac12}-g^{n+1}_{i-\frac12}}{\Delta x}\right\rangle=0, \tag{39}$$

with $M^n=M(U^n)$ *and* $\Pi_{i+\frac12}=\frac{\Pi(U_i)+\Pi(U_{i+1})}{2}$. *Then*
(i) in the limit ε *goes to zero, the moments* U^n *satisfy the following discretization of Euler equations*

$$\frac{U^{n+1}_i-U^n_i}{\Delta t}+\frac{F_{i+\frac12}(U^n)-F_{i-\frac12}(U^n)}{\Delta x}=0, \tag{40}$$

(ii) scheme (38)–(39) is asymptotically equivalent, up to $O(\varepsilon^2)$, *to the following scheme*

$$\frac{U^{n+1}_i-U^n_i}{\Delta t}+\frac{F_{i+\frac12}(U^n)-F_{i-\frac12}(U^n)}{\Delta x}$$
$$=\frac{\varepsilon}{\Delta x}\left\langle vm\Big[(I-\Pi^n_{i+\frac12})(v\ \frac{M^n_{i+1}-M^n_i}{\Delta x})-(I-\Pi^n_{i-\frac12})(v\ \frac{M^n_i-M^n_{i-1}}{\Delta x})\Big]\right\rangle, \tag{41}$$

which is a consistent approximation of the CNS equations (27). Moreover, the approximation of the diffusion term in the right-hand side of (41) is second order in space.

Proof. First part (i) is obvious. For (ii), the asymptotical equivalence between the two schemes up to $O(\varepsilon^2)$ is formally given by the above analysis. The fact that scheme (41) is consistent with the one dimensional CNS equations is just the result of a simple Taylor expansion for small Δt and Δx. The second order approximation of the diffusion term in (41) is due to the central differences and the symmetric discretization of $\Pi_M(x_{i+\frac12})$. □

Remark 4.1. In the case of coarse discretizations such that $\varepsilon<\Delta x$, the upwind approximation of the equilibrium flux $\partial_x F(U)$ gives a numerical viscosity (of order Δx) which is larger than the order ε physical viscosity. This is a classical issue for convection-diffusion problems with upwind approximation of the convection part. For not too small ε, it is often sufficient to use a second order approximation of $\partial_x F(U)$. In this paper, we use a simple reconstruction of the upwind flux $F_{i+\frac12}(U^n)$ based on a flux splitting $F=F^++F^-$ as sum of a positive and a negative part, following the idea in [7]. A standard second order approximation of $F_{i+\frac12}(U^n)$ is then given by a linear piecewise polynomial:

$$F^+(x)=F^+(x_i)+s_i(x-x_i),\quad \forall x\in[x_{i-\frac12},x_{i+\frac12}],$$

where a slope limiter is introduced to suppress possible spurious oscillations near discontinuities. For example, one can use the classical minmod slope limiter:

$$s_i = \frac{1}{\Delta x}\text{minmod}\left(F^+(U_{i+1}) - F^+(U_i), F^+(U_i) - F^+(U_{i-1})\right).$$

Finally, the numerical flux $F_{i+\frac{1}{2}}(U)$ is given as

$$F_{i+\frac{1}{2}}(U) = F_i^+(x_{i+\frac{1}{2}}) - F_{i+1}^-(x_{i+\frac{1}{2}}),$$

and $F_{i-\frac{1}{2}}(U)$ is reconstructed following the same way. Of course, here, the splitting form of the flux is naturally derived from its kinetic interpretation:

$$F(U) = \left\langle v^+ mM(U)\right\rangle + \left\langle v^- mM(U)\right\rangle.$$

5 Some standard numerical methods for solving the BGK equation

In this section, we compare our approach with some already known schemes to solve the BGK equation, regarding stability and asymptotic preserving properties. Following the notations given in section 4, we denote by $f_i^n(v)$ an approximation of $f(t_n, x_i, v)$, and by M_i^n the Maxwellian associated with f_i^n according to (9)-(10).

5.1 Explicit and semi-implicit schemes

The simplest time explicit scheme for the one dimensional BGK equation is written as

$$f_i^{n+1} = f_i^n - \frac{\Delta t}{\Delta x}\Big[v^+(f_i^n - f_{i-1}^n) + v^-(f_{i+1}^n - f_i^n)\Big] + \frac{\Delta t}{\varepsilon}(M_i^n - f_i^n). \tag{42}$$

Because of the stiff term $\varepsilon^{-1}(M_i^n - f_i^n)$, the stability of this scheme requires a CFL constraint of type $\Delta t = O(\varepsilon)$. Under this constraint, this scheme satisfies the standard physical properties: conservation of mass, momentum and energy, entropy dissipation, and preservation of positivity. However, it is clear that this scheme cannot be used for small ε, since it induces prohibitevely small time steps. In particular, this means that scheme (42) is not asymptotic preserving, neither for Euler, nor for CNS asymptotics.

In order to get a numerical scheme with a time step independent of ε, it is necessary to find a suitable time implicit discretization of the collision operator.

The simplest way is to make implicit the loss term $-\varepsilon^{-1}f$ only. Hence, we obtain the following discretization

$$f_i^{n+1} = \frac{\varepsilon}{\varepsilon + \Delta t} f_i^n - \frac{\Delta t}{\Delta x}\frac{\varepsilon}{\varepsilon + \Delta t}\Big[v^+(f_i^n - f_{i-1}^n) + v^-(f_{i+1}^n - f_i^n)\Big] + \frac{\Delta t}{\varepsilon + \Delta t} M_i^n. \tag{43}$$

Unlike the explicit scheme (42), scheme (43) does not has any ε dependent CFL condition, and satisfies the main physical properties of conservation and entropy.

However the limit scheme when ε goes to 0 is not consistent with the Euler equations. Indeed, when $\varepsilon \to 0$, (43) gives $f_i^{n+1} = M_i^n$ and hence $f_i^n = M_i^0$ for any time t_n.

5.2 The splitting method and its implicit version

The splitting method is the most frequently used procedure for solving kinetic equations both by deterministic and stochastic methods. It consists in using a time splitting between the transport and collision parts of the equation. The transport part is solved with the initial data f^n

$$\begin{aligned} &\partial_t \tilde{f} + v\ \partial_x \tilde{f} = 0 \quad t \in [t_n, t_{n+1}], \\ &\tilde{f}(t = t_n, x, v) = f^n(x, v), \end{aligned} \tag{44}$$

and then the relaxation part is solved by using $\tilde{f}(t_{n+1})$ as the initial data

$$\begin{aligned} &\partial_t \bar{f} = \frac{1}{\varepsilon}(M(\bar{U}) - \bar{f}), \quad t \in [t_n, t_{n+1}], \\ &\bar{f}(t = t_n, x, v) = \tilde{f}(t_{n+1}, x, v), \end{aligned} \tag{45}$$

and we set $f^{n+1} = \bar{f}(t_{n+1}, x, v)$. The convection phase (44) is approximated by an explicit scheme based on a finite difference method :

$$\frac{f_i^{n+\frac{1}{2}} - f_i^n}{\Delta t} + \frac{\Phi_{i+\frac{1}{2}}(f^n) - \Phi_{i-\frac{1}{2}}(f^n)}{\Delta x} = 0, \tag{46}$$

where the numerical flux is given by (33) and $f^{n+\frac{1}{2}}$ approximates $\tilde{f}(t_{n+1})$. For the collision phase, it is proposed in [8] to solve it exactly:

$$f_i^{n+1} = e^{-\frac{\Delta t}{\varepsilon}} f_i^{n+\frac{1}{2}} + (1 - e^{-\frac{\Delta t}{\varepsilon}}) M_i^{n+\frac{1}{2}}. \tag{47}$$

This scheme preserves the Euler limit since it gives for $\varepsilon = 0$ the following relation

$$\frac{U_i^{n+1} - U_i^n}{\Delta t} + \frac{F_{i+\frac{1}{2}}(U^n) - F_{i-\frac{1}{2}}(U^n)}{\Delta x} = 0,$$

where $F_{i+\frac{1}{2}}(U^n) = \left\langle m \Phi_{i+\frac{1}{2}}(M^n) \right\rangle$. This scheme is nothing but a kinetic scheme for the Euler equations. However, the CNS asymptotics cannot be preserved by this approach. Indeed, we note that since relation (47) is conservative, then $M_i^{n+\frac{1}{2}} = M_i^{n+1}$, and hence

$$f_i^{n+1} - M_i^{n+1} = e^{-\frac{\Delta t}{\varepsilon}}(f_i^{n+\frac{1}{2}} - M_i^{n+1}).$$

Therefore, the difference between f and its associated Maxwellian is smaller than any power of ε. In particular, this implies that there is no correction of order ε in the conservation laws. This means that the CNS asymptotics cannot be obtained with this scheme.

In order to obtain a CNS preserving splitting scheme, we propose the following modification. Instead of solving the collision step exactly, we discretize it by a simple forward difference:

$$\frac{f_i^{n+1} - f_i^{n+\frac{1}{2}}}{\Delta t} = \frac{1}{\varepsilon}(M_i^{n+\frac{1}{2}} - f_i^{n+1}). \tag{48}$$

In other words, this modification is equivalent to replace the coefficient $e^{-\frac{\Delta t}{\varepsilon}}$ by $\frac{1}{1+\Delta t/\varepsilon}$ in (47). As stated in the following proposition, scheme (46) and (48) is now able to recover the CNS asymptotics.

Proposition 5.1. *The numerical approximation of the one-dimensional BGK equation given by (46) and (48) is, up to $O(\varepsilon^2)$, equivalent to the following scheme*

$$\frac{U_i^{n+1}-U_i^n}{\Delta t}+\frac{F_{i+\frac{1}{2}}(U^n)-F_{i-\frac{1}{2}}(U^n)}{\Delta x} + \frac{\varepsilon}{\Delta x}\left(\left\langle m\left(\Phi_{i+\frac{1}{2}}(\frac{M^{n-1}-M^n}{\Delta t})-\Phi_{i-\frac{1}{2}}(\frac{M^{n-1}-M^n}{\Delta t})\right)\right\rangle-\frac{1}{\Delta x}\left\langle m\left(\Phi_{i+\frac{1}{2}}(D)-\Phi_{i-\frac{1}{2}}(D)\right)\right\rangle\right). \tag{49}$$

The fluxes $F_{i+\frac{1}{2}}$ and $\Phi_{i+\frac{1}{2}}$ are given by (35) and (33). The sequence D is defined as $D_i = \Phi_{i+\frac{1}{2}}(M^{n-1})-\Phi_{i-\frac{1}{2}}(M^{n-1})$.

This scheme is a consistent approximation of the CNS equations (27). Furthermore, the order ε term in (49) is an approximation of the diffusion term in (27) which is of the first order in Δx.

Proof. The consistency result is simply obtained by standard Taylor expansion at fixed ε. □

Now we discuss the differences between the AP scheme (38)–(39) obtained by the micro-macro decomposition and scheme (46)–(48) based on the splitting method. First, we note that the corresponding CNS numerical asymptotics (41) and (49) are not the same. Indeed, scheme (49) is a two-steps approximation (ie it uses U^{n+1}, U^n, and U^{n-1}). Moreover, the diffusion is discretized by a second order approximation in space in (41), while it is of first order only in (49). Note also that the approximation of the diffusion term in (49) induces an error of the order of Δt. No such error appears for scheme (41).

6 Numerical results

In this section, we present several numerical tests in the case of the one-dimensional BGK model. Our aim is to illustrate the efficiency of scheme (38)–(39) and to show its asymptotic equivalence up to $O(\varepsilon^2)$ to scheme (41). We also check the consistency of (41) with a standard approximation of the one-dimensional CNS equations (27). Finally, the behaviour of our schemes in the CNS regime is analyzed by comparing them with the following standard approximation of the CNS equations:

$$\frac{U_i^{n+1}-U_i^n}{\Delta t}+\frac{F_{i+\frac{1}{2}}(U^n)-F_{i-\frac{1}{2}}(U^n)}{\Delta x} = \frac{3\varepsilon}{2\Delta x^2}\begin{pmatrix} 0 \\ 0 \\ \frac{p_i+p_{i+1}}{2}(T_{i+1}-T_i)-\frac{p_{i-1}+p_i}{2}(T_i-T_{i-1}) \end{pmatrix}. \tag{50}$$

For clarity, we now fix some notations. We refer to scheme (38)–(39) obtained by the micro-macro decomposition as (AP), to the semi-implicit time splitting scheme given by (46) and (48) as (S_i), and to the time splitting scheme with exact collision phase given by (46)–(47) as (S_e). The CNS asymptotics (41) of scheme (AP) is refered to as $(AP1)$. The numerical scheme (40) for Euler equations is refered to as (E). We recall that this scheme is also the limit of the scheme (AP) when ε goes to 0. For these two schemes, the numerical convective fluxes $\partial_x F(U)$ are approximated by using the kinetic flux vector splitting (35). Finally, the standard scheme (50) for the CNS equations is refered to as (NS).

For all the schemes used in this section, the integrals with respect to the velocity are discretized by simple rectangle quadratures.

6.1 Stationary shock problem

We study in this section the one-dimensional stationary shock wave problem. The initial data is given by $f(0,x,v) = M[\rho,u,T]$ where the macroscopic quantities are left and right data connected by the classical Rankine-Hugoniot relations:

$$\begin{aligned} &\rho = 1, \quad u = 1.2, \quad T = 0.1 \quad \text{for } x < 0, \\ &\rho = 1.65, \quad u = 0.72, \quad T = 0.4 \quad \text{for } x > 0. \end{aligned}$$

This corresponds to a shock Mach number of 2.2. The computational domain in space is $[-7.5, 7.5]$ discretized with 200 cells, while the velocity space is truncated with the interval $[v_{min}, v_{max}] = [-3, 4]$ with 100 discrete points.

Our first purpose is to illustrate the behavior of scheme (AP) at different regimes. For different values of ε ($\varepsilon = 3^{-n}, n \geq 0$), we first plot the distribution function within the shock ($x = 0$) in figure 1. We also plot the density, the mean velocity, and the temperature as functions of $x \in [-7.5, 7.5]$ in figures (2)–(4). In each figure, we add the correspondig results obtained with the Euler limit scheme (E). These figures show that scheme (AP) is stable in the limit $\varepsilon = 0$ and converges to the correct Euler limit.

To check the behaviour of scheme (AP) in the kinetic regime, we compare in figure 5 the density obtained for $\varepsilon = 1$ with scheme (AP) and that obtained with the simple explicit discretization (42) of the BGK equation (denoted by $(BGKexp)$ in the figure). As expected, both schemes give the same results.

Now we illustrate the fact that the CNS asymptotics $(AP1)$ of scheme (AP) is indeed an approximation of the CNS equations (see the second assertion of proposition (4.3). The density obtained with scheme $(AP1)$ is compared for $\varepsilon = 1$ (kinetic regime), and $\varepsilon = 1.7 \times 10^{-5}$ (fluid regime) to the result obtained with the standard approximation (NS) of the CNS equations. In figure 6 we observe, as expected, that schemes (AP1) and (NS) give the same density profiles.

Then for schemes (AP) and (S_i), we numerically investigate the difference between their results and the Euler limit. We show that it is of the order of ε. We plot in figure 7 the relative differences between the densities, the velocities, and the temperatures, obtained with

schemes (AP) and (E), and with (S_i) and (E). As expected we observe that these profiles are lines with a slope equal to 1.

Finally, we numerically check that (AP) is asymptotically equivalent, up to $O(\varepsilon^2)$, to scheme $(AP1)$ for CNS equations at small ε. In figure 8 we plot the relative difference between the densities, the velocities, and the temperatures, obtained with schemes (AP) and (AP1). As expected, we obtain a line with a slope equal to 2. This is in very good agreement with the formal analysis given in the previous sections: it confirms that scheme (AP) accurately preserves the compressible Navier-Stokes asymptotics up to $O(\varepsilon^2)$.

6.2 Sod problem

In this section we consider the classical Sod problem with the following initial data for the density, mean velocity and temperature

$$(\rho, u, T) = \begin{cases} (1, 0, 1), & 0 \leq x \leq 0.5, \\ \\ (0.125, 0, 0.1), & 0.5 < x \leq 1. \end{cases}$$

The distribution function is initialized with the Maxwellian states corresponding to this data. The space domain $[0, 1]$ is discretized using 100 grid points, and the velocity domain $[-4.5, 4.5]$ is discretized with 100 points.

First, we consider scheme (AP). For different values of ε, we plot at time $t = 0.14$ and position $x = 0.5$ the distribution function in figure 9. We also plot in figures 10–12, at the same time and the same values of ε, the density, the velocity and the temperature. Again, these figures show that scheme (AP) is stable in the limit $\varepsilon = 0$ and converges to the correct Euler limit.

Finally, the differences between schemes that preserve the CNS asymptotics (i.e., (AP) and (S_i)) and a scheme that does not (ie (S_e)) are shown by plotting in figure 13 the rescaled heat flux $q = \frac{1}{\varepsilon}\left\langle \frac{|v-u|^2}{2}(v-u)f \right\rangle$. This quantity is obtained by scheme (AP), (S_i), and (S_e) and is compared to its theoretical asymptotic value $-\kappa\partial_x T$ obtained in scheme (NS), for $\varepsilon = 2 \times 10^{-3}$, $\varepsilon = 10^{-3}$ and $\varepsilon = 2 \times 10^{-4}$, at time $t = 0.16$. The time step is $\Delta t = 2 \times 10^{-3}$. According to the theory given in section 4 and 5, q should be of order 1 for (NS) and for the asymptotic preserving schemes (AP) and (S_i), while it should be of order $e^{-\Delta t/\varepsilon}/\varepsilon$ for (S_e). Indeed, we observe in figure 13 that the heat flux given by (S_e) is smaller than the one given by the other schemes, and even much smaller for $\varepsilon = 10^{-4}$. Comparatively, scheme (AP) gives a heat flux which becomes close to that given by the CNS discretization (NS) when ε decreases. Finally, our modified splitting scheme (S_i) is also close to (NS), but it shows some oscillations that are probably due to the complex discretization of the diffusion term in (49).

7 Conclusion

In this paper, we have presented a numerical method for kinetic Boltzmann equations which preserves the CNS asymptotics at small Knudsen numbers. The key ingredient in this method is to use an equivalent micro-macro formulation of the kinetic equation. This formulation has been discretized with a numerical scheme which is uniformly stable with respect to the Knudsen number and turns out to be efficient in both kinetic and fluid regimes. This has been illustrated by several numerical tests for the one-dimensional BGK model.

We have also presented a simple modification of a classical splitting approach for the BGK equation which leads to the same asymptotic preserving property (for the CNS asymptotics). We mention that, at least for a particular class of quadratic Boltzmann operators, a similar modification on the so-called Wild sums [14] could be made to obtain CNS asymptotic preserving schemes using splitting techniques. This work is currently under consideration [2].

However, the method based on the micro-macro decomposition seems to be more natural and should more easily extend to other collision operators (Boltzmann, Landau, etc.). This is the subject of a future work. The treatment of boundary conditions in the micro-macro decomposition is also under consideration. Moreover, we mention that this approach has already been applied to obtain asymptotic preserving schemes in the diffusion limit for linear kinetic equations [24].

References

[1] C. Bardos, F. Golse, and D. Levermore. Fluid dynamic limits of kinetic equations. I. Formal derivations. *J. Statist. Phys.*, 63(1-2):323–344, 1991.

[2] M. Bennoune, M. Lemou, and L. Mieussens. in preparation.

[3] R.-E. Caflisch, S. Jin, and G. Russo. Uniformly accurate schemes for hyperbolic systems with relaxation. *SIAM J. Numer. Anal.*, 34(1):246–281, 1997.

[4] C. Cercignani. *The Boltzmann equation and its applications*, volume 67 of *Applied Mathematical Sciences*. Springer-Verlag, New York, 1988.

[5] C. Cercignani. *Rarefied gas dynamics*. Cambridge Texts in Applied Mathematics. Cambridge University Press, Cambridge, 2000. From basic concepts to actual calculations.

[6] S. Chapman and T.-G. Cowling. *The mathematical theory of non-uniform gases. An account of the kinetic theory of viscosity, thermal conduction and diffusion in gases*. Third edition, prepared in co-operation with D. Burnett. Cambridge University Press, London, 1970.

[7] H. Choi and J.-G. Liu. The reconstruction of upwind fluxes for conservation laws: its behavior in dynamic and steady state calculations. *J. Comput. Phys.*, 144(2):237–256, 1998.

[8] F. Coron and B. Perthame. Numerical passage from kinetic to fluid equations. *SIAM J. Numer. Anal.*, 28(1):26–42, 1991.

[9] N. Crouseilles, P. Degond, and M. Lemou. A hybrid kinetic/fluid model for solving the gas dynamics Boltzmann-BGK equation. *J. Comput. Phys.*, 199(2):776–808, 2004.

[10] P. Degond and S. Jin. A smooth transition model between kinetic and diffusion equations. *SIAM J. Numer. Anal.*, 42(6):2671–2687 (electronic), 2005.

[11] P. Degond, S. Jin, and L. Mieussens. A smooth transition model between kinetic and hydrodynamic equations. *J. Comput. Phys.*, 209(2):665–694, 2005.

[12] P. Degond and M. Lemou. On the viscosity and thermal conduction of fluids with multivalued internal energy. *Eur. J. Mech. B Fluids*, 20(2):303–327, 2001.

[13] P. Degond, J.-G. Liu, and L. Mieussens. Macroscopic fluid models with localized kinetic upscaling effects. *Multiscale Model. Simul.*, 5(3):940–979 (electronic), 2006.

[14] E. Gabetta, L. Pareschi, and G. Toscani. Relaxation schemes for nonlinear kinetic equations. *SIAM J. Numer. Anal.*, 34(6):2168–2194, 1997.

[15] S. Jin. Efficient asymptotic-preserving (AP) schemes for some multiscale kinetic equations. *SIAM J. Sci. Comput.*, 21(2):441–454 (electronic), 1999.

[16] S. Jin and C.-D Levermore. Numerical schemes for hyperbolic conservation laws with stiff relaxation terms. *J. Comput. Phys.*, 126(2):449–467, 1996.

[17] S. Jin and L. Pareschi. Discretization of the multiscale semiconductor Boltzmann equation by diffusive relaxation schemes. *J. Comput. Phys.*, 161(1):312–330, 2000.

[18] S. Jin and L. Pareschi. Asymptotic-preserving (AP) schemes for multiscale kinetic equations: a unified approach. In *Hyperbolic problems: theory, numerics, applications, Vol. I, II (Magdeburg, 2000)*, volume 141 of *Internat. Ser. Numer. Math., 140*, pages 573–582. Birkhäuser, Basel, 2001.

[19] A. Klar. An asymptotic-induced scheme for nonstationary transport equations in the diffusive limit. *SIAM J. Numer. Anal.*, 35(3):1073–1094 (electronic), 1998.

[20] A. Klar. An asymptotic preserving numerical scheme for kinetic equations in the low Mach number limit. *SIAM J. Numer. Anal.*, 36(5):1507–1527 (electronic), 1999.

[21] A. Klar. A numerical method for kinetic semiconductor equations in the drift-diffusion limit. *SIAM J. Sci. Comput.*, 20(5):1696–1712 (electronic), 1999.

[22] A. Klar and C. Schmeiser. Numerical passage from radiative heat transfer to nonlinear diffusion models. *Math. Models Methods Appl. Sci.*, 11(5):749–767, 2001.

[23] P. Le Tallec and F. Mallinger. Coupling Boltzmann and Navier-Stokes equations by half fluxes. *J. Comput. Phys.*, 136(1):51–67, 1997.

[24] M. Lemou and L. Mieussens. A new asympotic preserving scheme base on micro-macro decomposition for linear kinetic equations in the diffusion limit. submitted.

[25] J.-C. Mandal and S.-M. Deshpande. Kinetic flux vector splitting for Euler equations. *Comput. & Fluids*, 23(2):447–478, 1994.

[26] G. Naldi and L. Pareschi. Numerical schemes for kinetic equations in diffusive regimes. *Appl. Math. Lett.*, 11(2):29–35, 1998.

[27] L. Pareschi and R.-E. Caflisch. An implicit Monte Carlo method for rarefied gas dynamics. I. The space homogeneous case. *J. Comput. Phys.*, 154(1):90–116, 1999.

[28] L. Pareschi and G. Russo. Time relaxed Monte Carlo methods for the Boltzmann equation. *SIAM J. Sci. Comput.*, 23(4):1253–1273 (electronic), 2001.

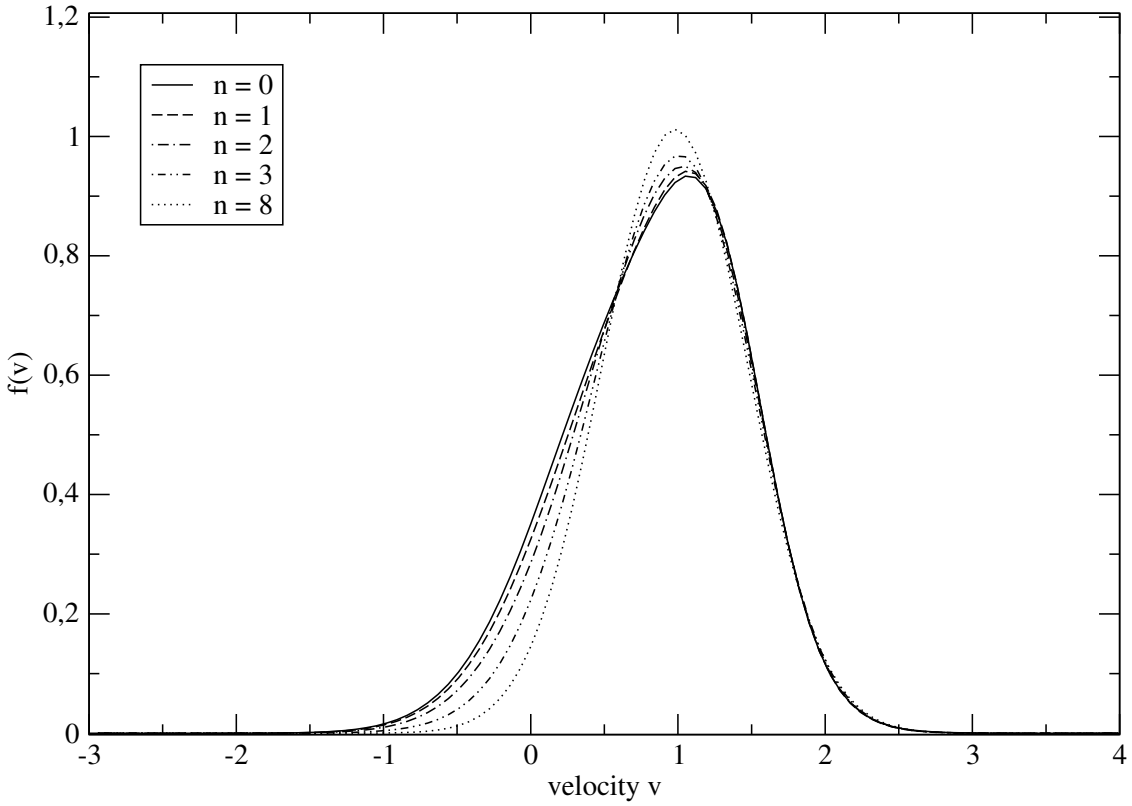

Figure 1: Stationary shock: distribution function f within the shock ($x = 0$) as a function of the velocity $v \in [-3, 4]$ given by scheme (AP). Profiles of f for different values of $\varepsilon_n = 3^{-n}$ for rarefied regime ($\varepsilon_0 = 1, \varepsilon_1 = 0.333, \varepsilon_2 = 0.11$), intermediate regime ($\varepsilon_3 = 3.7 \times 10^{-2}$) and fluid regime ($\varepsilon_8 = 1.52 \times 10^{-4}$) where f becomes close to a Maxwellian.

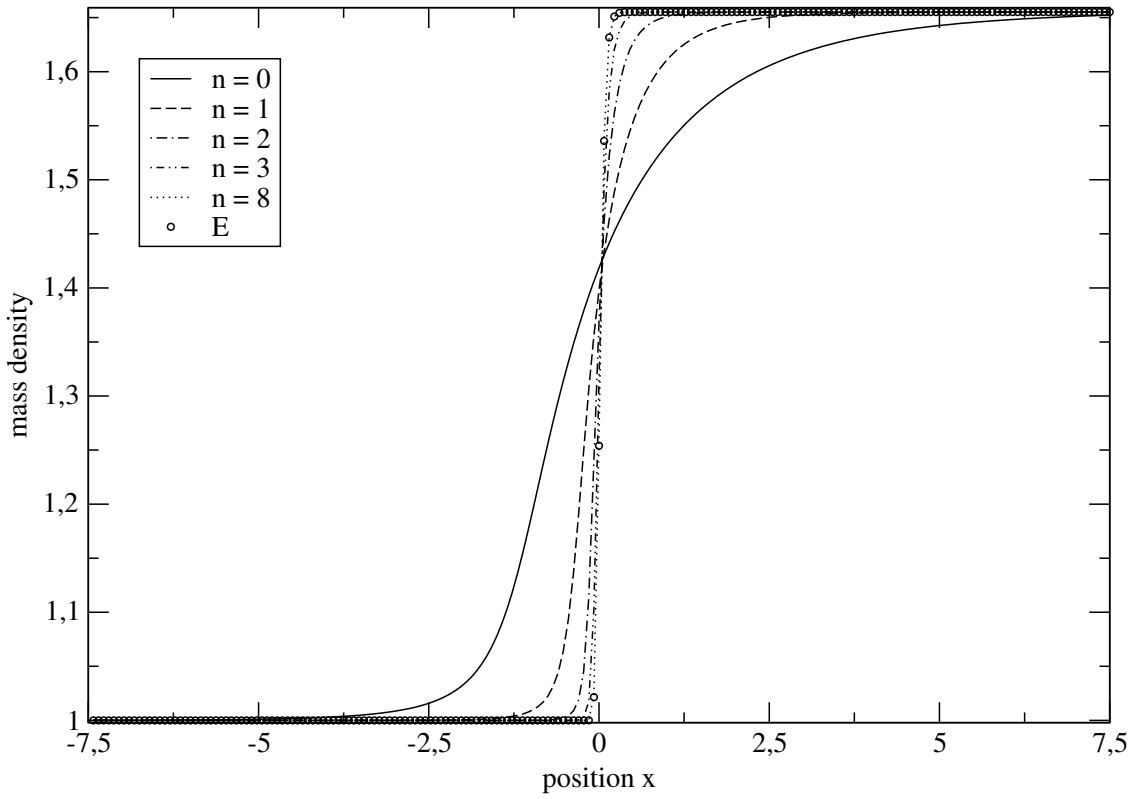

Figure 2: Stationary shock: mass density as a function of the position $x \in [-7.5, 7.5]$ given by scheme (AP). Profiles of ρ for different values of $\varepsilon_n = 3^{-n}$ for rarefied regime $(\varepsilon_0 = 1, \varepsilon_1 = 0.333, \varepsilon_2 = 0.11)$, intermediate regime $(\varepsilon_3 = 3.7 \times 10^{-2})$ and fluid regime $(\varepsilon_8 = 1.52 \times 10^{-4})$. The result of scheme (E) is also shown.

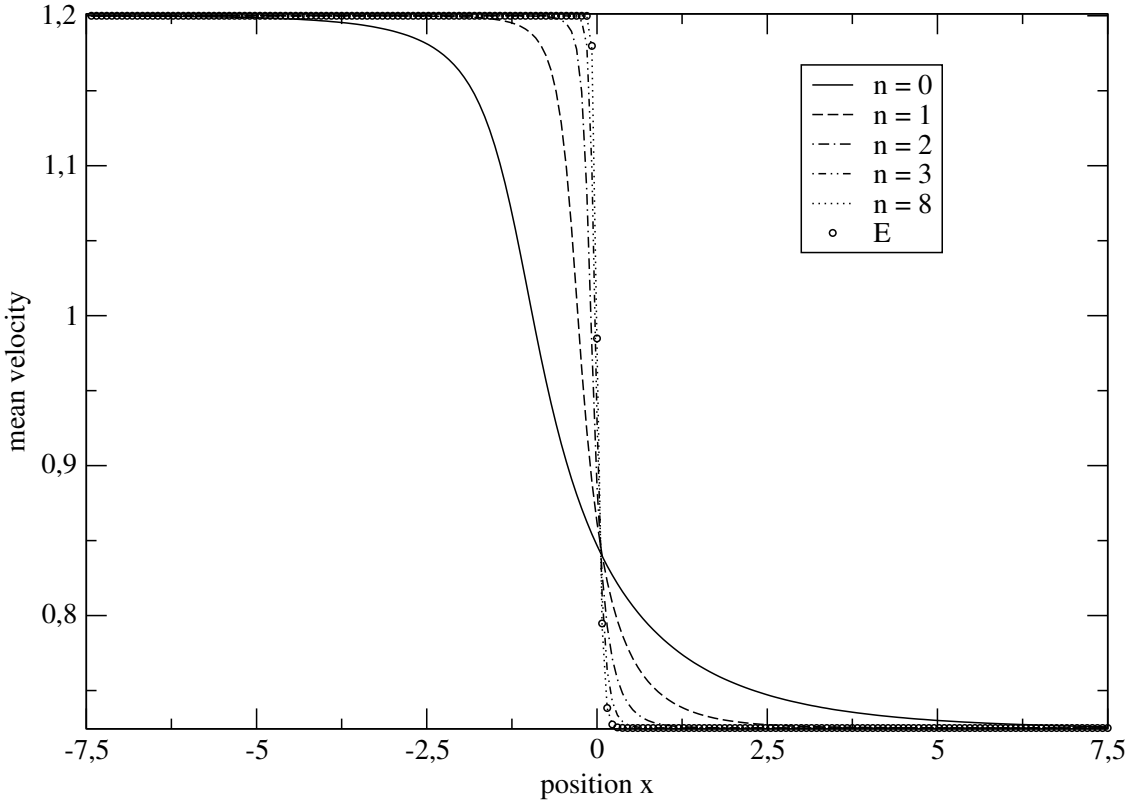

Figure 3: Stationary shock: mean velocity as a function of the position $x \in [-7.5, 7.5]$ given by scheme (AP). Profiles of u for different values of $\varepsilon_n = 3^{-n}$ for rarefied regime ($\varepsilon_0 = 1, \varepsilon_1 = 0.333, \varepsilon_2 = 0.11$), intermediate regime ($\varepsilon_3 = 3.7 \times 10^{-2}$) and fluid regime ($\varepsilon_8 = 1.52 \times 10^{-4}$). The result of scheme (E) is also shown.

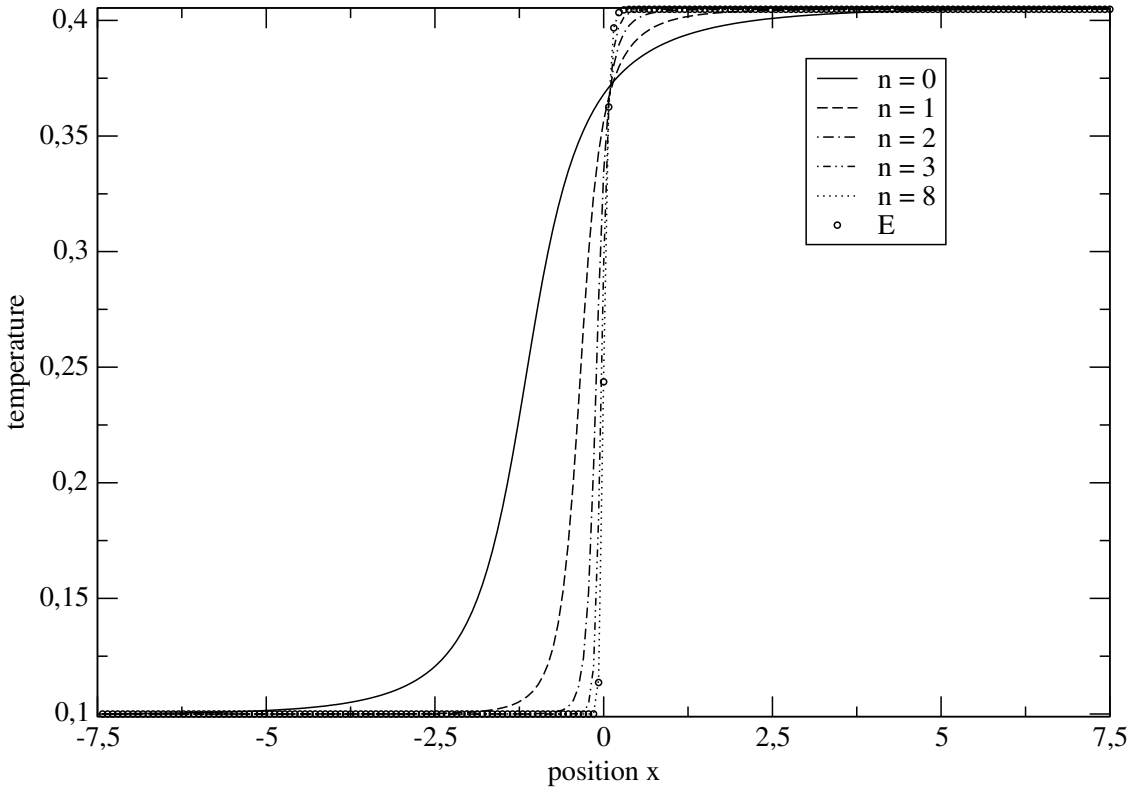

Figure 4: Stationary shock: temperature as a function of the position $x \in [-7.5, 7.5]$ given by scheme (AP). Profiles of T for different values of $\varepsilon_n = 3^{-n}$ for rarefied regime ($\varepsilon_0 = 1, \varepsilon_1 = 0.333, \varepsilon_2 = 0.11$), intermediate regime ($\varepsilon_3 = 3.7 \times 10^{-2}$) and fluid regime ($\varepsilon_8 = 1.52 \times 10^{-4}$). The result of scheme (E) is also shown.

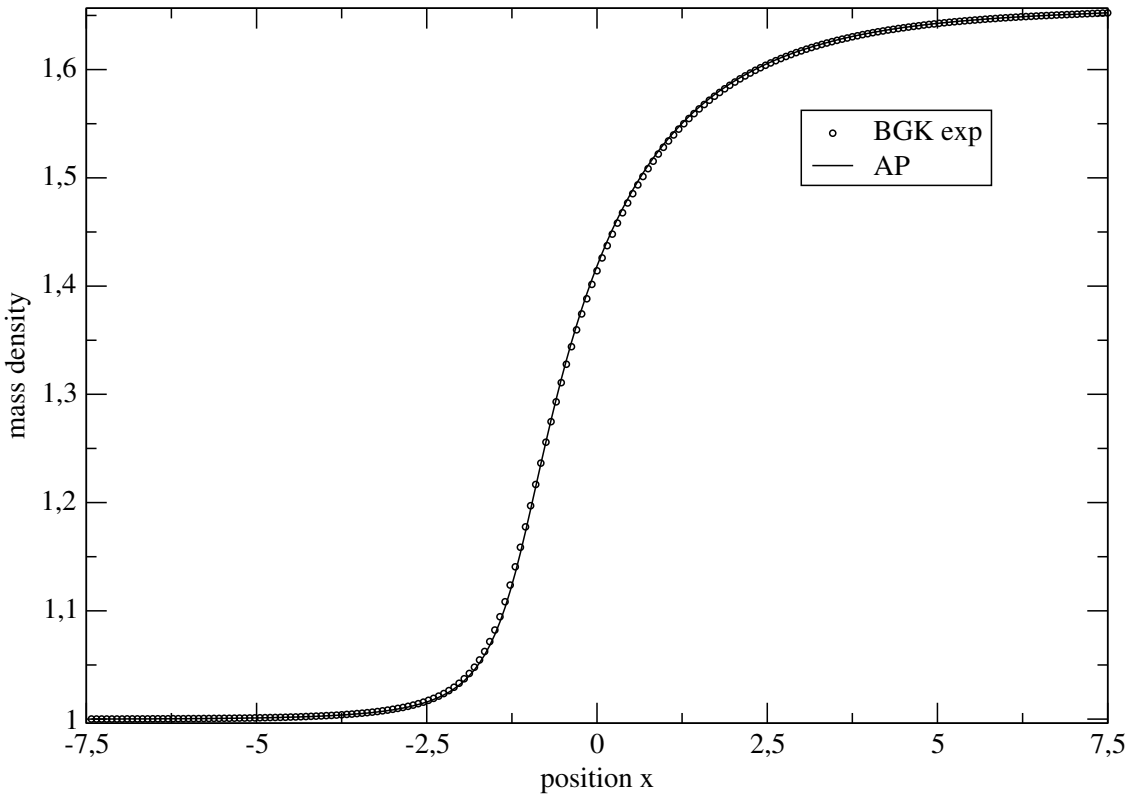

Figure 5: Stationary shock: mass density as a function of the position $x \in [-7.5, 7.5]$ for $\varepsilon = 1$ (rarefied regime) obtained by schemes $(BGKexp)$, and (AP).

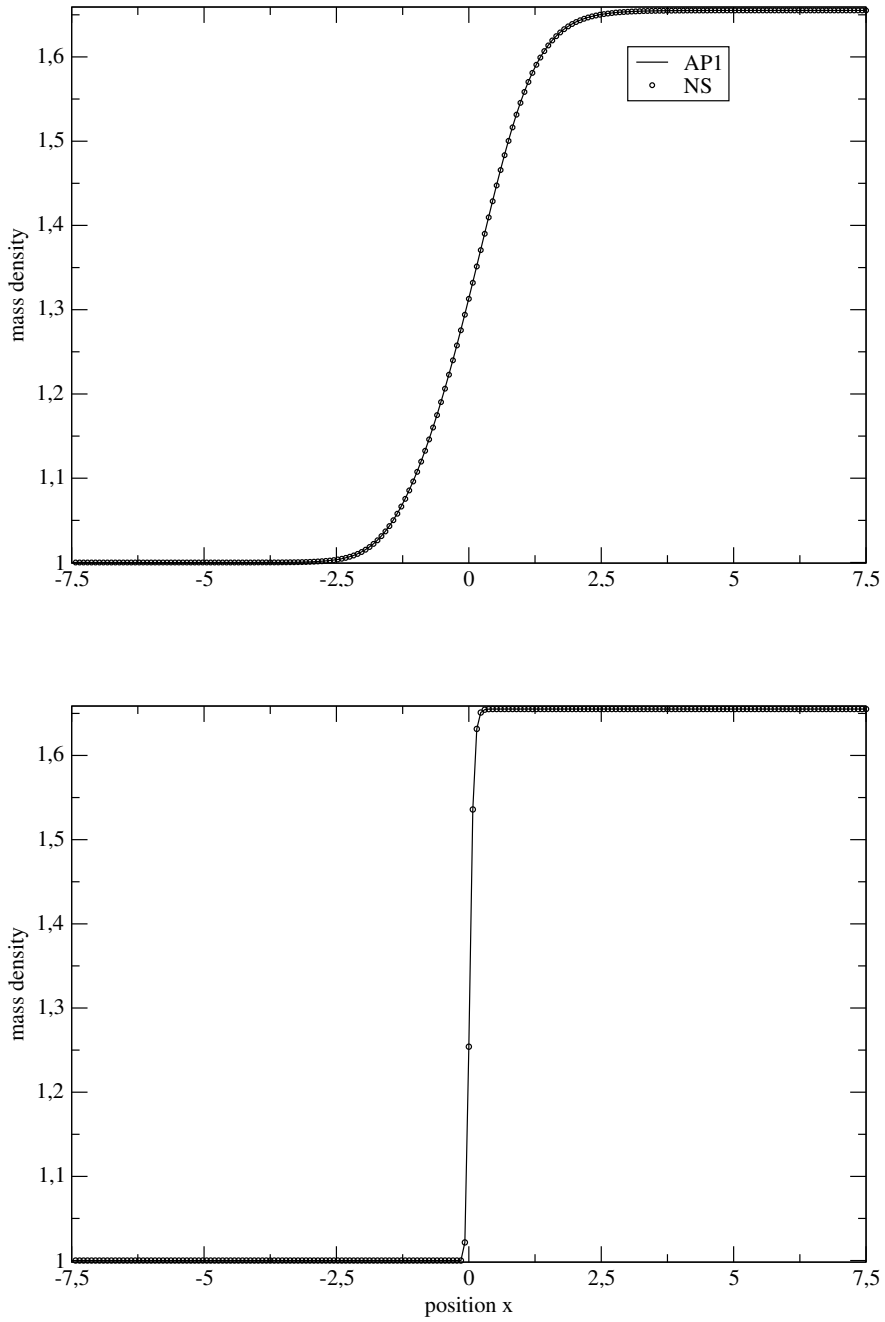

Figure 6: Stationary shock: mass density as a function of the position $x \in [-7.5, 7.5]$ for $\varepsilon = 1$ (rarefied regime, top) and for $\varepsilon = 2.32 \times 10^{-8}$ (fluid regime, bottom) obtained by schemes $(AP1)$ and (NS).

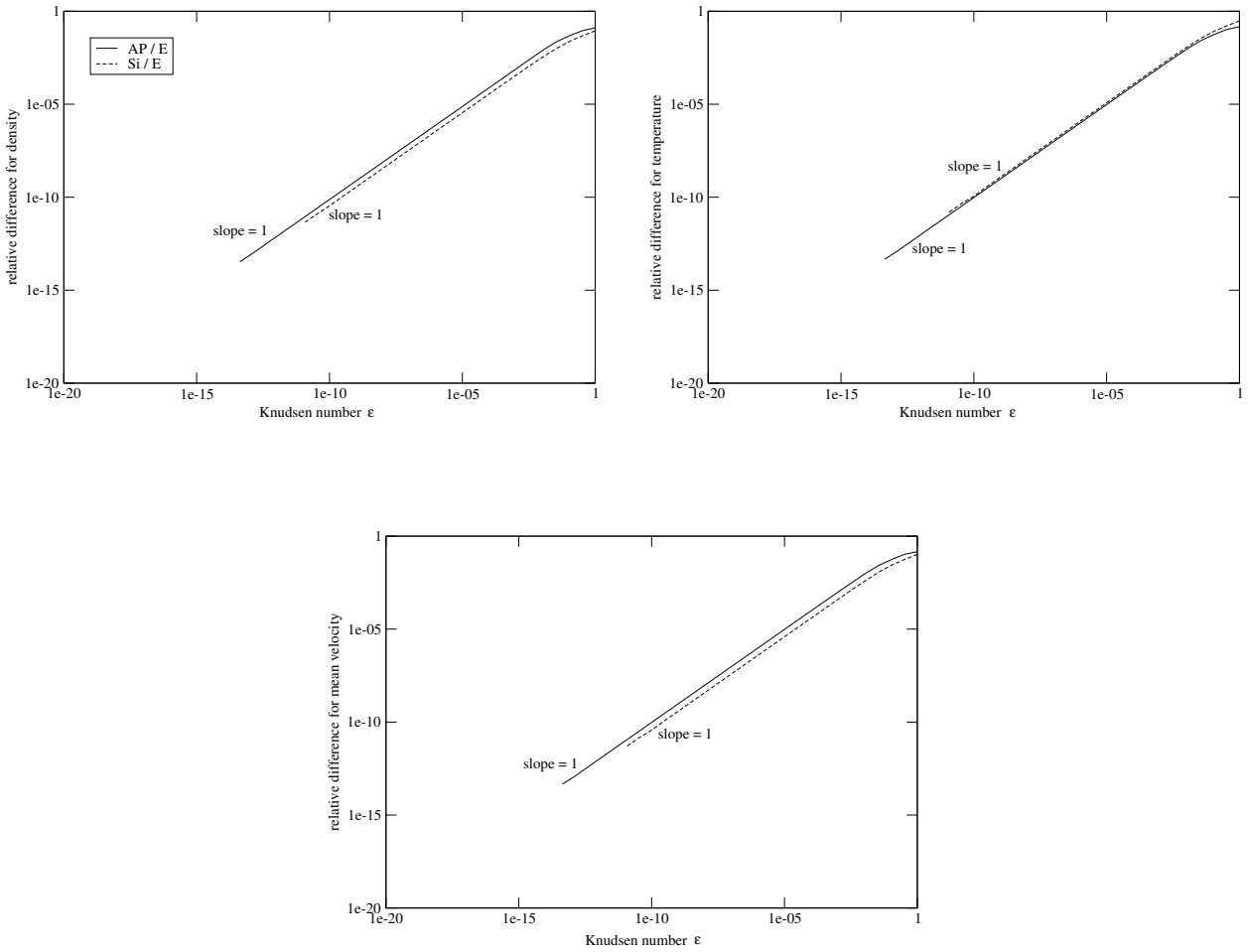

Figure 7: Stationary shock: relative differences (in log scale) between the densities (top left), the velocities (top right), and the temperatures (bottom), obtained with schemes (AP) and (E), and with (S_i) and (E). Different values are considered: $\varepsilon_n = 3^{-n}, n = 0, 1, \cdots 28$.

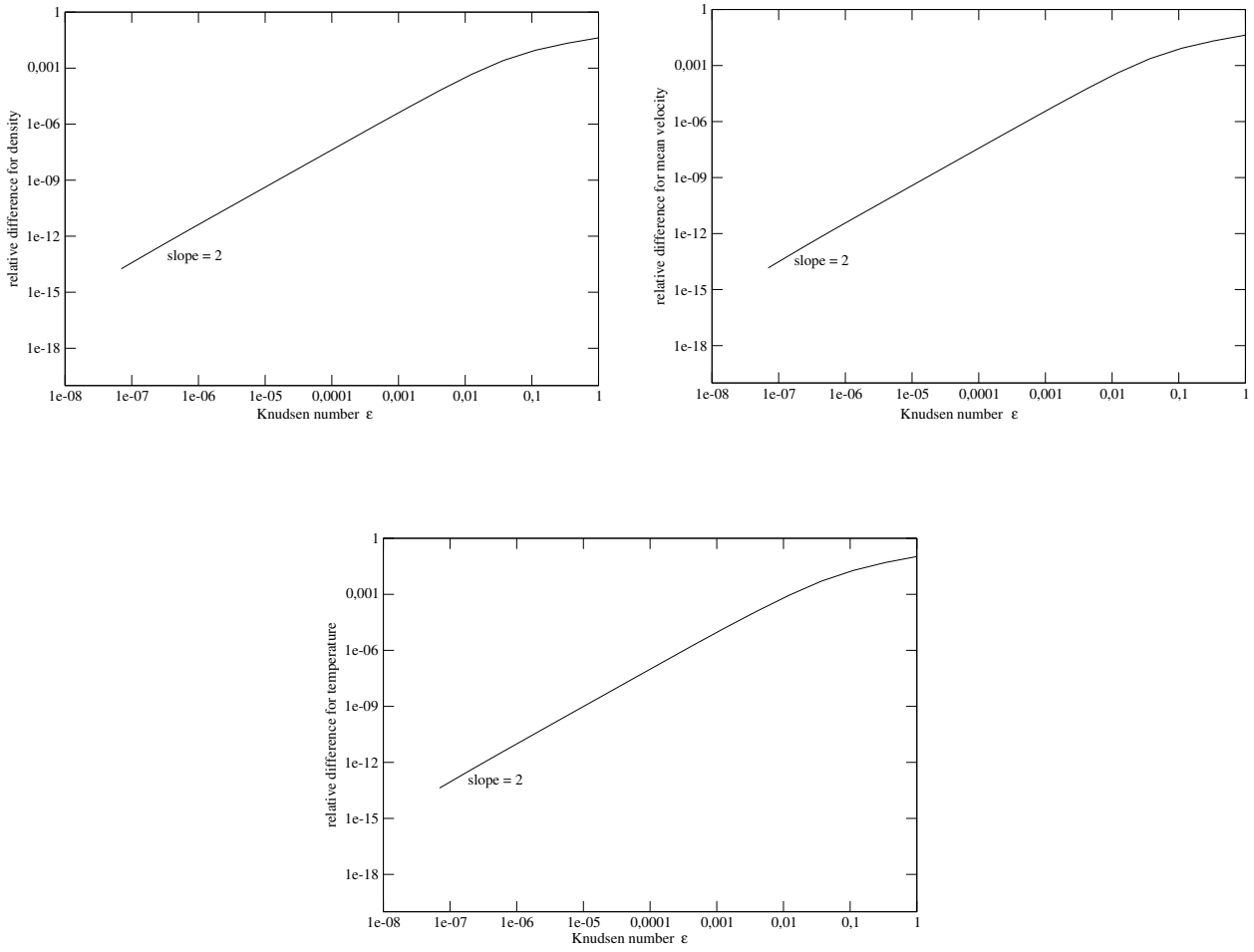

Figure 8: Stationary shock: relative differences (in log scale) between the densities (top left), the velocities (top right), and the temperatures (bottom), obtained with schemes (AP) and $(AP1)$. Different values are considered: $\varepsilon_n = 3^{-n}, n \geq 0$.

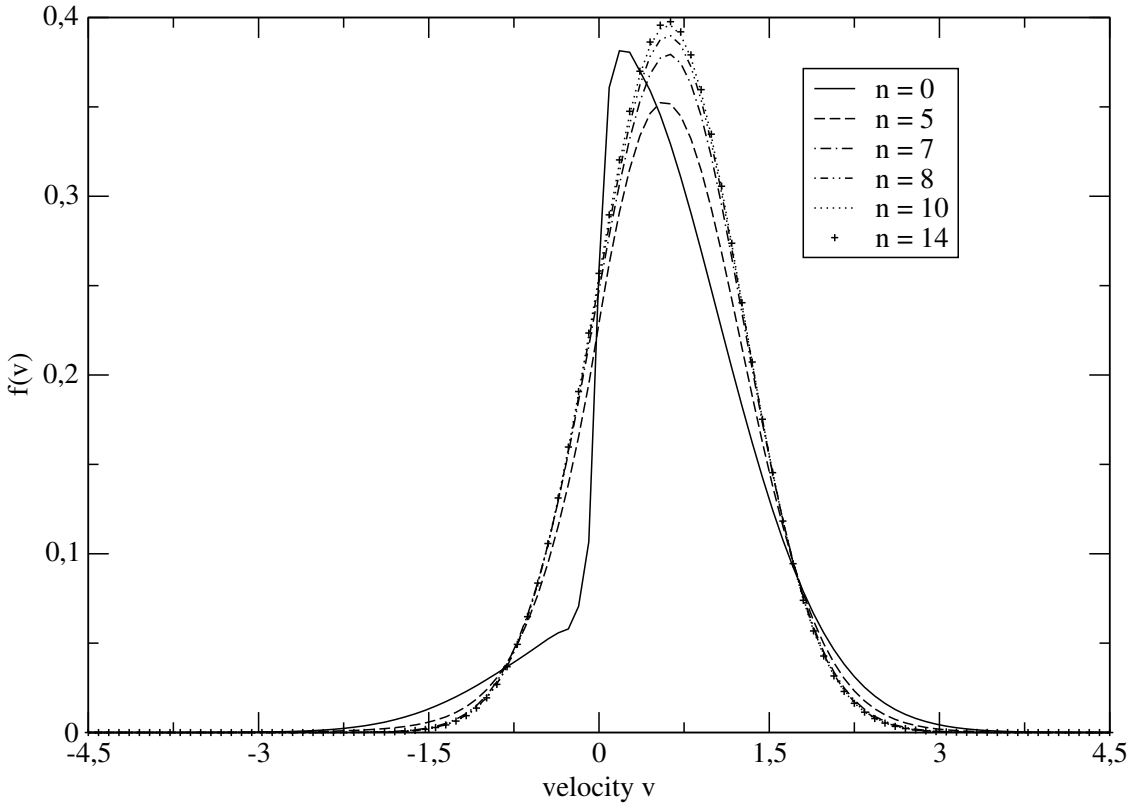

Figure 9: Sod problem: distribution function f at point $x = 0.5$ as a function of the velocity $v \in [-4.5, 4.5]$ given by scheme (AP) at time $t = 0.14$. Profiles of f for different values of $\varepsilon_n = 2^{-n}$ in rarefied regime ($\varepsilon_0 = 1, \varepsilon_5 = 3.125 \times 10^{-2}$), transition regime ($\varepsilon_8 = 3.90 \times 10^{-3}$) and fluid regime ($\varepsilon_{10} = 9.7 \times 10^{-4}, \varepsilon_{14} = 6.10 \times 10^{-5}$) where f becomes close to a Maxwellian.

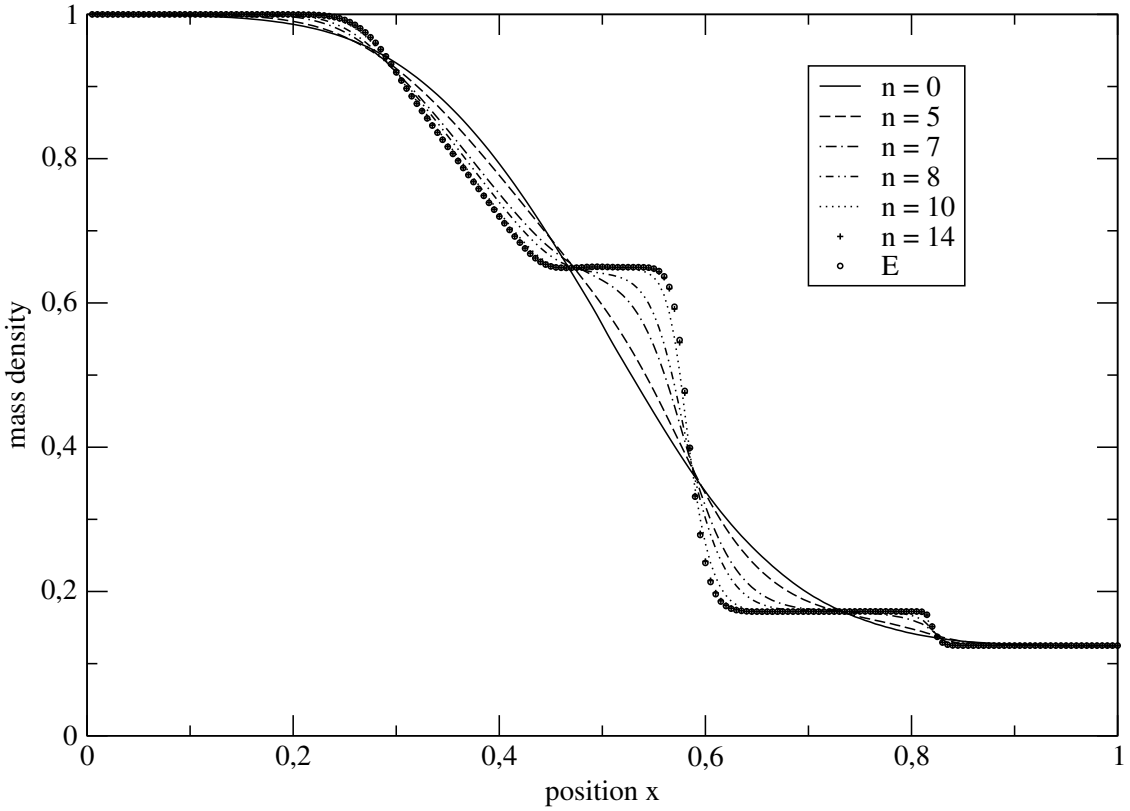

Figure 10: Sod problem: mass density as a function of $x \in [0,1]$ at time $t = 0.14$, given by scheme (AP). Profiles for different values of $\varepsilon_n = 2^{-n}$ for rarefied regime ($\varepsilon_0 = 1, \varepsilon_5 = 3.125 \times 10^{-2}$), transition regime ($\varepsilon_8 = 3.90 \times 10^{-3}$) and fluid regime ($\varepsilon_{10} = 9.7 \times 10^{-4}, \varepsilon_{14} = 6.10 \times 10^{-5}$). The result of scheme (E) is also shown.

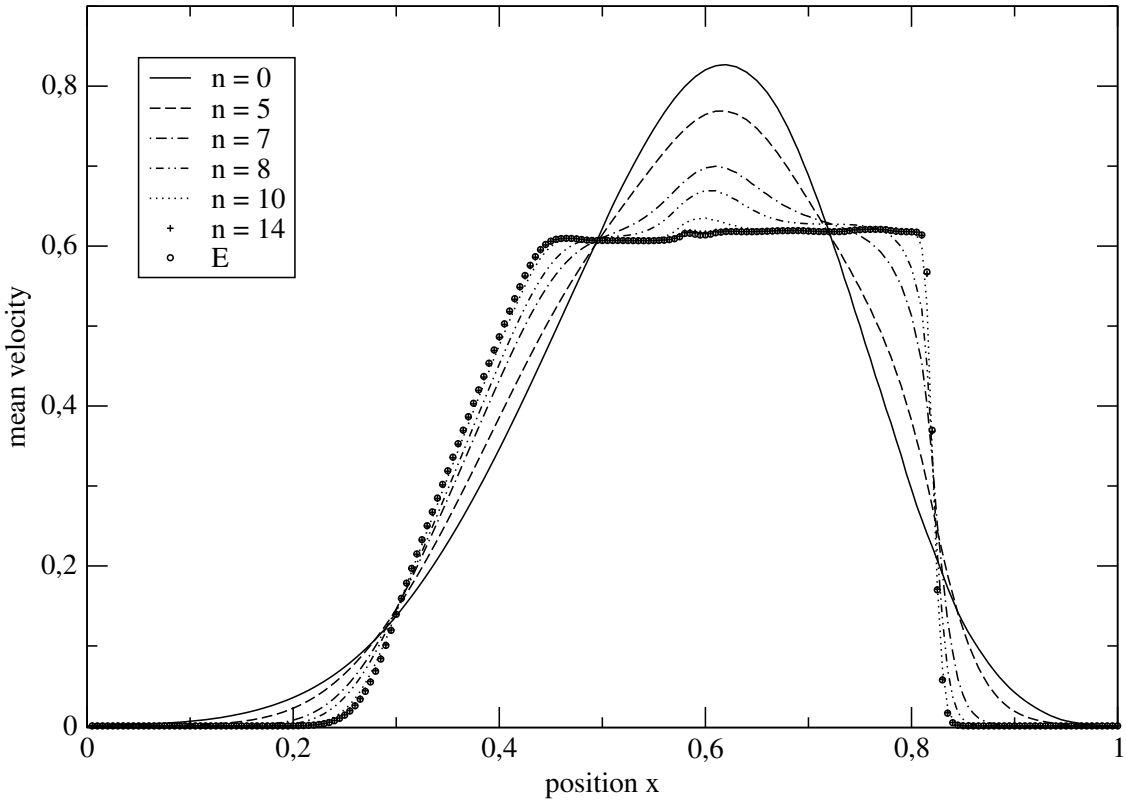

Figure 11: Sod problem: mean velocity as a function of $x \in [0,1]$ at time $t = 0.14$, given by scheme (AP). Profiles for different values of $\varepsilon_n = 2^{-n}$ for rarefied regime ($\varepsilon_0 = 1, \varepsilon_5 = 3.125 \times 10^{-2}$), transition regime ($\varepsilon_8 = 3.90 \times 10^{-3}$) and fluid regime ($\varepsilon_{10} = 9.7 \times 10^{-4}, \varepsilon_{14} = 6.10 \times 10^{-5}$). The result of scheme (E) is also shown.

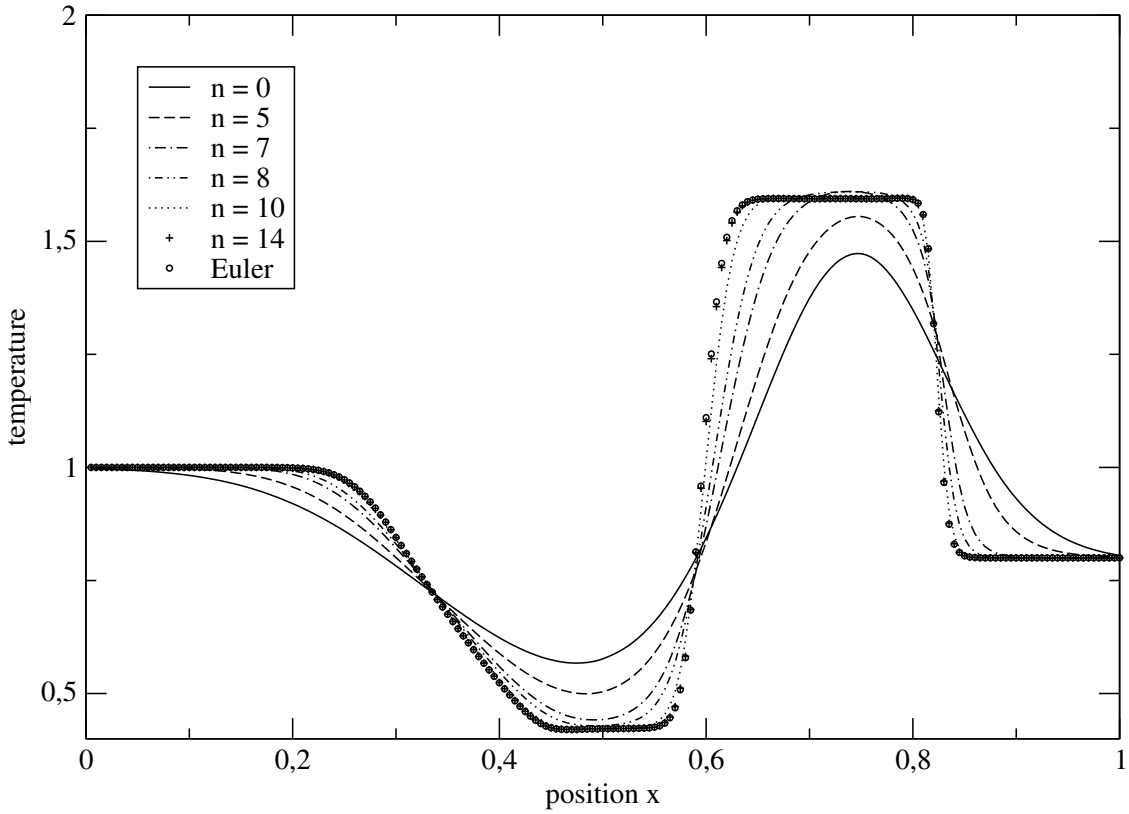

Figure 12: Sod problem: temperature as a function of $x \in [0,1]$ at time $t = 0.14$, given by scheme (AP). Profiles for different values of $\varepsilon_n = 2^{-n}$ for rarefied regime ($\varepsilon_0 = 1, \varepsilon_5 = 3.125 \times 10^{-2}$), transition regime ($\varepsilon_8 = 3.90 \times 10^{-3}$) and fluid regime ($\varepsilon_{10} = 9.7 \times 10^{-4}, \varepsilon_{14} = 6.10 \times 10^{-5}$). The result of scheme (E) is also shown.

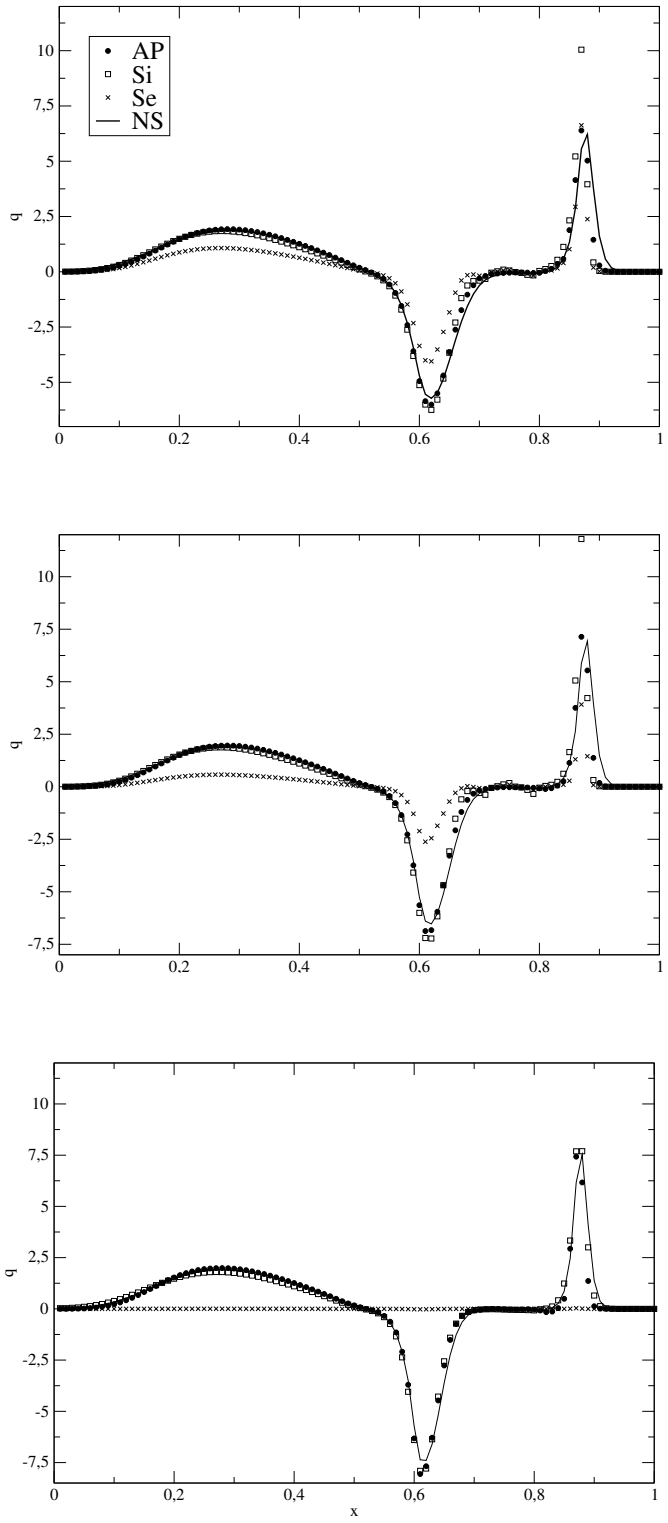

Figure 13: Sod problem: heat flux scaled by ε as a function of $x \in [0,1]$ for schemes (AP), (S_i) (that preserve CNS asymptotics), for scheme (NS) and for scheme (S_e). Time $t = 0.16$, and $\varepsilon = 2^{-9} \approx 2 \times 10^{-3}$ (top), $\varepsilon = 2^{-10} \approx 10^{-3}$ (middle) and $\varepsilon = 2^{-12} \approx 2 \times 10^{-4}$ (bottom).